Environmental and Experimental Botany 165 (2019) 1–18

Contents lists available at ScienceDirect

Environmental and Experimental Botany

journal homepage: www.elsevier.com/locate/envexpbot

Prediction and validation of DREB transcription factors for salt tolerance in *Solanum lycopersicum* L.: An integrated experimental and computational approach

Krishna Kumar Rai[a,b], Nagendra Rai[a,*], Shashi Pandey Rai[b]

[a] Indian Institute of Vegetable Research, Post Box-01, P.O.-Jakhini (Shahanshahpur), Varanasi, 221305 Uttar Pradesh, India
[b] Centre of Advance Study, Department of Botany, Institute of Science, Banaras Hindu University (BHU), Varanasi, 221005 Uttar Pradesh, India

ARTICLE INFO

Keywords:
DREB1
KYRG domain
Homology modelling
Salt stress
DNA-protein interaction

ABSTRACT

The dehydration responsive element binding (DREB) transcription factors (TFs) have been intensely reported to regulate plant growth and defence response under stress condition. In this study, we have investigated impact of salt stress (400 mM) at vegetative stage in tomato hybrids on (1) several yield and related components (2) relative water content, membrane stability (3) enzymatic activity and gene expression levels of stress responsive genesand since in tomato, little is known about its functional binding motifs, protein-protein interactions and core amino acid residues involved in the regulation of its expression under stress condition (4)we also used in silico approach to structurally and functionally characterize tomato DREB1 protein in response to salt stress. Salt stress imposed at vegetative stage caused significant reduction in relative water content, chlorophyll content, proline content, expression of stress responsive genes and enhanced membrane damage in all the hybrids. However, hybrids *viz.,* VRTH-1754 and VRTH-1755 showed remarkable tolerance to salt stress as they showed low membrane damage, increased proline content and enhanced activity of antioxidant enzyme along with expression of stress responsive genes. Phylogenetic foot-printing, multiple sequence alignment, and motif analysis of *S. lycopersicum* DREB1 (SlDREB1) reveal remarkable similarities with its wild homologue showing monophyletic origin with *S. pimpinellifolium* and close relation with *S. pennelli* and *S. tuberosum*. Additionally, DNA-protein interaction study revealed that the SlDREB1 protein binds to Dehydration Responsive Element (DRE) DNA element through conserved KYRG region of AP2/ERF domain with flanking sequences *viz.,* Tyr^{49}, Gly^{50}, Pro^{51}, Cys^{52}, and Arg^{54}.Furthermore, gene ontology (GO) analysis predicted the most significant subcellular localization of SlDREB1 protein to the chloroplast (32.9%) followed by nucleus (28.9%) and cytoplasm (17.6%) revealing that SlDREB1 proteins were mainly involved in ethylene mediated signalling pathway, transcription initiation and defence response.

1. Introduction

Sessility is one of the most noxious features of plants that imposes severe threat to their survival under variable environmental conditions such as high/low temperatures, drought, salinity and UV radiations (Xin et al., 2014). Among all, soil salinity is one of the major environmental constraint that limit crop growth, yield that ultimately affects agricultural productivity and is projected to have devastating effect on global food production in coming years (Xin et al., 2014). According to an estimate, 77 million hectares of land (out of 1.5 billion hectares of total world arable land) will become unsuitable for crop growth because of increasing land salinization due to universal climate change and outrageous irrigation practises (Erskine et al., 2014). So, in order to adapt and survive under these environmental fluctuations,-plants activatecomplex multi-fold mechanisms of stress adaptive signalling cascades thereby triggering dynamic and temporal reprogramming of complex network of proteins called transcription factors (TFs). Transcription factors are trans-acting predominate class of genes that strategically regulate crop growth under stress conditions upon binding specifically to *cis*-acting elements (promoter) and activating the transcription of defence related genes(Hichri et al., 2014).TFs are also known to integrates multitude of synergistic/antagonistic signalling networks of several other TFs and functional genes thus improving plant's phenotypical and physiological adaptability under stress conditions.

Among various TFs, Dehydration responsive element binding

* Corresponding author.
E-mail address: nrai1964@gmail.com (N. Rai).

https://doi.org/10.1016/j.envexpbot.2019.05.015
Received 22 April 2019; Received in revised form 24 May 2019; Accepted 25 May 2019
Available online 29 May 2019

(DREB) proteinis the most important and best studied subfamily of TFs, belonging to largest group *viz.*, APETALA 2/Ethylene Responsive Element Binding Factor (AP2/ERF) plant-specific transcription factors family which is involved in the mitigation of abiotic stress induced oxidative damagesby regulating the expression of genes involved in stress defence pathway (Pandey et al., 2014). DREBs proteins are also well documented toprovide immunity against several biotic stresses by modulating the expression of several downstream genes of defence signalling cascades through feed backward-forward loop mechanisms (Muneer and Jeong, 2019). In addition, DREBs are also exclusively involve in the induction of salinity tolerance by acting downstream of auxin and ethylene signalling pathways and upstream of ABA-independent signalling pathway thereby reprogramming transcriptional activation of DELLA nuclear proteins that are involvedin the regulation of plant growth under salinity stress (Hichri et al., 2016).

In tomato, DREB proteins are recognised by the presence of highly conserved YRG (˜20 amino acids in length) region/elements in their AP2/ERF DNA binding domain that contain ˜60 amino acids, with highly conserved short hexapeptide KYRGVR motif at N terminus, have been proposed to be involve in DNA binding activity (Park et al., 2016). Second, LAYD region which is ˜18 amino acids long at C-terminus capable of mediating protein-protein interaction and thus forming an amphipathic alpha helix with ability to regulate DNA binding activity of DREBs by instigating significant change in the conformation of YRG elements (Muchate et al., 2016). The highly conserved YRGVR residues of the core motif with arginine and tryptophan residues in beta sheet together with two conserved functional amino acids *viz.,* valine and glutamic acid residues are crucial for interaction with phosphate backbone of Dehydration Responsive Element (DRE) of nine base pairs conserved DNA sequence 5′-TACCGACAT-3′ (Kazan, 2015). The DRE motif was originally identified in drought responsive promoter of *rd29A* gene as well as from the nuclear extracts of salt stressed protein factors of *Arabidopsis* plants and the sequence of which was confirmed by gel-shift assay (Dey and Corina Vlot, 2015).

In the past recent years, extensive studies have been done to assess the role of stress inducible DREBs transcription factors in the regulation of gene expression in response to various abiotic stresses (Sun et al., 2015; Guo et al., 2016; Wang et al., 2016). They have been shown to transcriptionally activate the ectopic expression of defence related genes involved in host defence mechanisms in *Arabidopsis* (Chen et al., 2016), tobacco (Mishra et al., 2015), potato (Charfeddine et al., 2015).The studies in these crops have laid the ground on which DREB has emerged as a key gene (compared to its corresponding counterparts *viz.,* WRKY, MYB, MYC and NAC) having potential to confer multiple abiotic stress tolerance upon its transcriptional reprograming (Wang et al., 2016).However, only few studies have investigated the role of DREBs in response to salinity stress tolerance in tomato (Rao et al., 2015a; Hichri et al., 2016), which mainly focuses on physiological, biochemical, gene expressionand microarray analysis.

Knowledge about DNA binding motif, functional domain, conserved amino acid residues involved in the regulation of stress tolerance regarding their biological and molecular function in tomato is scarce. So, in this study, our objectives were to (a) characterize tomato hybrids for their physio-biochemical ability to tolerate salt stress, (b) determinethe expression level of DREB1 candidate genes for salt tolerance in selected tomato hybrids and (c) to unravel DNA-protein interaction, protein-protein interaction, gene ontology enrichment analysis using *in-silico* approach to explore probable residues involved in DNA protein binding and functional interactive partners involved in DREB1 signalling. In addition, comprehensive knowledge about binding motifs, key residues, active sites and probable ligand binding sites can help predicts biological, molecular and functional dimensions of DREB1 protein which are crucial for modulation of stress tolerance in tomato plants.

2. Materials and methods

2.1. Plant materials and growth condition

An experiment was designed to decipher the consequences of salinity stress in four tomato hybrids *viz.,* VRTH-1747, VRTH-1749, VRTH-1754 and VRTH-1755 along with KT-8 variety (salt tolerant variety) and Agata-30 (salt enduring variety) as a check under green-house conditions at Indian Institute of Vegetable Research Varanasi (U.P), India from September to December 2017. Both of these varieties has been used as a one of the donor parents in the development of all the four hybrids. The parents were selected on the basis of their initial screening i.e. seed germination percentage in basic nutrient solution containing 200 mM of NaClunder *in-vitro* condition (Supporting information Figure S1). Seeds of all the hybrids along with parents were sown in the beginning of September and seedlings with 4–5 true leaves were transplanted in polyvinyl chloride pots (20 and 16 cm in diameter) filled with 5000 g of air-dried soil organized by mixing loam soil with farm yard manure (FYM) in 1:3 v/v quantity. The approximate day and night conditions during the entire experimental period were 28–32 °C/18-26 °C air temperature, 1050–1450 μmol/m^2s light intensity and 40–50% relative humidity.

2.2. Experimental design and stress exposure

Salt treatments of 400 mM NaCl were initiated in the mid October, when the inflorescence appeared form each seedling growing uniformly. The NaCl (400 mM) was applied in four treatments which was repeated at three days interval till the optimum concentration of NaCl was achieved. The pH of all NaCl treated soil as well as soil from control pots were measured using digital pH meter: for NaCl treated soils the pH ranged from 7.62 to 7.92 whereas in control soils the pH ranged from 6.52 to 6.72, respectively. All the plants were divided randomly in to three sets with ten pots in each set (Supporting information Figure S2).One set was used as control, second set was used for various physiological, biochemical and molecular analysis after the completion of the treatment, while third set was left for four more weeks to observe growth parameters and fruit quality attributes.Each set with 10 pots was considered as single replicate, therefore there were thirty pots in three replicates. The fully-expanded third leaf from the top was plucked on the completion of the treatment, frozen immediately in liquid N_2, and kept at −80 °C until further analysis.

2.3. Measurement of indicators for photosynthetic function

Measurement of photosynthetic function was done in terms of relative water content (RWC)andphotosynthetic pigment contents. Relative water content was measured by recording fresh weight (FW), turgid weight (TW) and dry weight (DW) of 15 uniform sized leaf discs devoid of midrib following the method of Turner and Kramer (1980) and was measured as per the following equation: Leaf RWC (%) = [(FW-DW)/ (TW-DW)] × 100. Total chlorophyll and carotenoid contents were measured by extracting leaf tissue in 80% acetone (Porra et al., 1989) and recording the absorbance of supernatant at 663, 645, 480 and 510 nm. The amount of photosynthetic pigments in leaf samples were computed as per the equation given by Arnon (1949) and expressed as mg g^{-1}FW.

2.4. Measurement of indicators for membrane damage

Electrolytic leakage and lipid peroxidation as an indicator for membrane damage. Electrolytic leakage was measured by recording the conductivity of 15 leaf leachates at 40 and 100 °C using conductivity meter (Century Instruments, Chandigarh, India). The conductivities were determined by following the standard equation: (C1/C2) × 100 (Deshmukh et al., 1991). Lipid peroxidation was determined by

measuring the absorbance of malondialdehyde (MDA) level at 532 nm and 600 nm generated by the reaction between thiobarbituric acid and trichloroacetic acid using the method of Heath and Packer (1968).

2.5. Measurement of indicators for oxidative stress

Hydrogen peroxide content, proline content and catalase activity were measured as an indicator of oxidative stress from both salt-affected and unaffected leaf tissue. Hydrogen peroxide (H_2O_2) content was measured by recording the strength of yellow coloured solution containing 50 mm phosphate buffer (pH 6.5), and 1 ml of 0.1% titanium sulfate in 20% H_2SO_4 at 410 nm (Jana and Choudhuri, 1981). Proline level was examined by extracting leaf tissue in 3% sulfosalicylic acid and recording the absorbance of chromophore containing acid ninhydrin at 520 nm (Bates et al., 1973). Activity of antioxidative enzyme catalase was assayed by homogenizing leaf tissues in 50 mM Tris NaOH buffer (pH 8.0) containing PVP, Triton X-100 and EDTA and recording the absorption of assay mixture for 5 min at 240 nm (Mckersie et al., 1990). The activity was expressed in μmol of H_2O_2 oxidized min^{-1} mg^{-1} protein.

2.6. RNA isolation and cDNA preparation

TRIZOL reagent (Invotrogen) was used to isolate total RNA following the manufacturer's instructions. The intensity of the isolated RNA was confirmed by recording the absorption ratio at 260/280 nm between 1.80 and 2.05 and 260/230 nm ranging from 2.00 to 2.60 using Nanophotometer (Implen, California, USA) and integrity was confirmed on 1.0% agarose gel electrophoresis tinged with ethidium bromide. The isolated RNA was then used to synthesise first strand of cDNA using 1.0 μg of RNA and the iScriptTM cDNA synthesis kit (Bio-Rad Laboratories, USA), according to manufacturer's instructions.

2.7. Real time (RT-PCR) gene expression analysis

Real time PCR analysis was performed only on one tomato hybrid i.e. VRTH-17-55 because it has superior physiological and biochemical adaptability to salt stress compared to its corresponding counterparts along with better yield related attributes.SsoFast™EvaGreen®Supermix detection chemistry (Bio-Rad) was used for the real time PCR analysis using iQ5thermocycler (BioRad Laboratories, USA). Primers were designed by accessing the sequences from Genbank using Primer 3 software (Supporting information Table 1) and the reactions were formulated in an overall volume of 20 μl containing: 1 μl of each gene specific primers (0.2 μM) and 10 μl of 2 × SsoFast™EvaGreen® Supermix and 2 μl of the template (20 ng). The relative quantification was done by using the $2^{-\Delta\Delta CT}$ method given by Livak and Schmittgen (2001) and was further normalized to the C_t data of *ACTIN* transcript level as an internal control. Each gene per sample was analysed for at least three biological and three technical replicates. Data obtained from RT-PCR were subjected to Bio-conductor R (http://www.bio conductor.org) analysis to generate heat map.

2.8. Database search and comparative phylogeny

Tomato dehydration responsive element binding 1 (DREB 1) protein (Locus: NP_001234689.1) was retrieved from NCBI database and NCBI BLAST server http://blast.ncbi.nlm.nih.gov/Blast.cgi was used to identify functional and relevant sequential homologue with in the other members of solanaceous family. The sequences were selected on the basis of percentage identity, query cover, E value.The sequences having sequence identity (> 90%) were selected for sequential classification and phylogenetic study.The alignment of the sequences was checked using Bio-Edit tool (Hall, 1999) and phylogenetic tree was constructed by employing UPGMA method with 1000 bootstrap replications values using MEGA 7 suite http://www.megasoftware.net (Tamura et al., 2013). Sequential classification between all the identified members of DREB protein sequences were inferred by performing multiple sequence alignment using CLC bio workbench and the functional DREB domain regions occupied by DREB proteins were identified by using InteProScanhttp://www.ebi.ac.uk/Tools/pfa/iprscan (Jones et al., 2014), NCBI CDD server http://www.ncbi.nlm.nih.gov/Structure/cdd/cdd.shtml (Marchler-Bauer et al., 2011) and ExPASy-Prosite scan http://prosite.expasy.org/scanprosite (de Castro et al., 2006). The distribution of conserved motifs in DREB 1 protein present across all the identified members was investigated using MEME Suite 4.1.1.2 (Multiple EM for Motif Elicitation) http://meme.ncbr.net (Bailey et al., 2006). The selection parameter for motif analysis was set to any number of repeats with motif width of 10 and 30 residues and maximum number of motifs to be analysed was set to 40. The circos visualization tool http://circos.ca (Krzywinski et al., 2009) was used for the identification of similarities and differences for the characterized DREB 1 protein with the different members of tomato family using percentage similarity matrices obtained through Clustal W phylogenetic clustering program.

2.9. Gene prediction and promoter analysis

The gene prediction analysis was done to find out all the available DREB members present in the genome of tomato. The protein sequence of DREB1 was subjected to TBLASTN search using whole genome shortgun contigs (wgs) with organism name *S. lycopersicum* (taxid: 4081). The BLAST results obtained were further subjected to Fgenesh (HMM based gene prediction tool) server http://www.softberry.com for identification and predicting the position of DREB1 protein across the whole tomato genome (Solovyev et al., 2006). The nucleotide sequences encoding DREB1 protein was identified and characterized on the basis of transcriptional start site and Poly A sequences. Further, gene display server (GSDS 2.0) http://gsds.cbi.pku.edu.cn/ (Hu et al., 2014) was used for the structural characterization of DREB1 gene which was also confirmed by subjecting protein sequences relevant to the nucleotide sequences to BLAST-P against uniport database.

2.10. Structural modelling and validation

The identified protein sequences for DREB1 protein in tomato were taken for homology modelling and DNA protein docking analysis. The template proteins for modelling DREB1 protein were identified using BLAST-P programme of Protein Data Bank (http://www. rcsb.org/pdb) (Berman et al., 2000). Four most closely related protein templates (confirmed by evaluating them on several other platforms using BLAST-P programme of NCBI) whose crystal structures were resolved through NMR and X-ray diffraction were used to generate 3D structure of proteins using MODELLER module of Discovery studio 3.0 (accelrys.com; Shahi et al., 2013). The MODELLER generated four models based on the available templates i.e. complex of GCC-box binding domain of ATERF1 (PDB ID: 1GCC), Crystal Structure of AtERF96 with GCC-box (PDB ID: 5WX9), solution structure of the GCC-box binding domain (PDB ID: 2GCC) and solution structure of the GCC-box binding domain (PDB ID: 3GCC). The selected modelled protein was further refined for Cα traces using two-step atomic level energy minimization module of ModRefiner http://zhanglab.ccmb.med.umich.edu/ModRefiner (Xu and Zhang, 2011) and topological details of the modelled protein was retrieved by superimposing the modelled proteins with each templates using Superpose version 1.0 http://wishart.biology.ualberta.ca/superpose (Maiti et al., 2004). The structural stability and reliability of the predicted models were further checked on several qualitative and quantitative score values and the model with the lowest energy values was selected for further study. The qualitative assessments of the models were done in terms of geometric analysis of the models, stereochemical orientation and patterns of backbone conformations of nonbonded atomic interactions. Single model method was use for the qualitiative estimation of predicted model using ProSA https://prosa.services.came.

Table 1
Changes in physiological and biochemical parameters in tomato hybrids/parents subjected to 400 mM of salt stress.

Hybrids/parents	Treatments	RWC (%)	EL (%)	Chlorophyll ($mgg^{-1}fw$)	Carotenoid ($mgg^{-1}fw$)	LPO ($mMg^{-1}fw$)	Proline ($\mu gg^{-1}gfw$)	H_2O_2 ($\mu mg^{-1}gfw$)	Catalase ($\mu mol\ H_2O_2$ oxidized $min^{-1}\ mg^{-1}$ protein)
VRTH-17-55	Control	86.4 ± 0.86 ^{a}	17.6 ± 0.52^{b}	5.98 ± 0.21 ^{ab}	2.16 ± 0.19 ^{ab}	1.33 ± 0.16^{c}	14.4 ± 0.49^{a}	1.14 ± 0.24^{c}	3.19 ± 0.20 ^{a}
	400 mM	83.8 ± 0.33^{a}	18.0 ± 0.47^{cd}	5.62 ± 0.25^{a}	2.17 ± 0.16^{a}	2.10 ± 0.09^{cd}	35.8 ± 0.71^{b}	2.85 ± 0.38^{d}	8.54 ± 0.28 ^{a}
VRTH-17-47	Control	80.1 ± 0.77 ^{ab}	18.5 ± 0.60 ^{b}	5.57 ± 0.28 ^{bc}	2.09 ± 0.16 ^{ab}	1.70 ± 0.17^{b}	13.8 ± 0.58 ^{ab}	2.18 ± 0.31^{b}	2.57 ± 0.20 ^{b}
	400 mM	78.3 ± 0.46^{b}	19.5 ± 0.52^{c}	4.42 ± 0.20^{b}	2.10 ± 0.16^{a}	2.94 ± 0.14^{b}	29.7 ± 0.35 ^{c}	3.58 ± 0.20^{c}	7.06 ± 0.20 ^{b}
VRTH-17-54	Control	85.5 ± 0.59 ^{a}	15.3 ± 0.53^{c}	6.11 ± 0.13 ^{a}	2.25 ± 0.19 ^{a}	1.21 ± 0.07^{c}	15.1 ± 0.29 ^{a}	1.55 ± 0.14^{c}	2.69 ± 0.12 ^{b}
	400 mM	79.0 ± 0.32 ^{b}	16.6 ± 0.44^{d}	5.81 ± 0.16 ^{abc}	2.19 ± 0.22^{a}	1.91 ± 0.19^{d}	42.3 ± 0.68^{a}	2.88 ± 0.16^{d}	7.73 ± 0.43 ^{ab}
VRTH-17-49	Control	84.6 ± 0.96 ^{a}	19.3 ± 0.44 ^{ab}	5.81 ± 0.27 ^{a}	1.93 ± 0.13 ^{bc}	1.69 ± 0.08 ^{b}	11.1 ± 0.41^{c}	2.12 ± 0.13^{b}	1.93 ± 0.12^{c}
	400 mM	78.5 ± 0.40^{b}	22.2 ± 0.49^{b}	3.58 ± 0.09^{c}	1.46 ± 0.20^{b}	3.11 ± 0.20^{b}	32.6 ± 0.44^{c}	4.57 ± 0.28^{b}	3.97 ± 0.22 ^{c}
KT-8 (Salt tolerant)	Control	79.0 ± 0.87 ^{b}	18.1 ± 0.46 ^{b}	5.45 ± 0.28 ^{c}	2.12 ± 0.20 ^{ab}	1.66 ± 0.16^{b}	12.5 ± 0.48^{bc}	2.75 ± 0.14 ^{a}	3.32 ± 0.16^{a}
	400 mM	73.6 ± 0.61^{c}	21.4 ± 0.47^{b}	4.59 ± 0.20^{b}	1.96 ± 0.24^{a}	2.26 ± 0.13^{c}	25.6 ± 0.71^{d}	5.39 ± 0.28^{a}	7.14 ± 0.22 ^{b}
Agata-30 (Salt enduring)	Control	72.1 ± 0.74 ^{c}	21.3 ± 0.46 ^{a}	4.39 ± 0.19 ^{d}	1.76 ± 0.11 ^{c}	1.87 ± 0.12^{a}	9.10 ± 0.40^{d}	2.67 ± 0.23 ^{a}	1.94 ± 0.19^{c}
	400 mM	68.5 ± 0.44^{d}	32.4 ± 0.66^{a}	3.70 ± 0.19^{c}	1.22 ± 0.15^{b}	3.55 ± 0.27^{a}	13.6 ± 0.38^{e}	4.66 ± 0.20^{b}	3.71 ± 0.23^{c}
Two-Way Anova									
Genotype		***	***	***	***	***	***	***	***
Environment		***	***	***	***	***	***	***	***
Genotype × Environment		NS	***	***	**	***	***	*	***

The values of relative water content (RWC), electrolytic leakage (EL), chlorophyll, carotenoid, lipid peroxidation (LPO), proline, hydrogen peroxide (H2O2) and catalase (means of three replicates ± SE) in the same column with different letters are significantly different at the 0.05 level according to Duncan's multiple range test from each other ($P < 0.05$). Data were analysed with two-way ANOVA. *$P < 0.05$; **$P < 0.01$; ***$P < 0.001$; NS; not significant.

sbg.ac.at/ (Wiederstein and Sippl, 2007), Qmean https://swissmodel.expasy.org/qmean/ (Benkert et al., 2009), RESPROX (Resolution by Proxy), ERRAT http://services.mbi.ucla.edu/ERRAT/stats/ (Colovos and Yeates, 1993) whereas quantitative evaluation was made using VADAR (Volume, Area, Dihedral Angle Reporter) http://vadar.wishartlab.com/analysis (Willard et al., 2003). Ramachandran plot was used for evaluation of backbone conformations of the predicted model by measuring the backbone dihedral phi (φ) and psi (Ψ) angles using PROCHECK module of PDBSum server http://www.ebi.ac.uk/pdbsum/ (Laskowski et al., 2005) and further confirmed by RAMPAGE server http://mordred.bioc.cam.ac.ik/~rapper/rampage.php (Lovell et al., 2003). Furthermore, reliability of our predicted model was also confirmed on ProTSAVmetaserver http://www.scfbio-iitd.res.in/software/proteomics/protsav.jsp (Singh et al., 2016) that utilizes different validation tools to validate the correctness of the structural model based on the global quality score values. The protein models generated for the functional domain were further submitted to an online repository of PMDB (Castrignano et al., 2006) to obtain the accession identities.

2.11. DNA-protein interaction

The molecular docking studies between GCC box and the DREB 1 protein sequence was done using Hex 8.0 molecular docking server (Macindoe et al., 2010). The parameters used for protein and ligand interaction study was correlation type i.e. Shape + Electro + DARS, FFT Mode-3D fast lite and grid range of 0.6 with Receptor: Ligand: Twist: Distance range of 180: 180: 360: 40. The docked complex having lowest binding energy values was analysed DS Studio 3.0 for identification of key residues involved in the interaction with the DNA.

2.12. Protein-protein interaction, structural and functional annotation

The functional protein-protein interactive partners involved in DREB 1 signalling cascades and biological pathway at both cellular and molecular level was analysed through STRING server (Search Tool for the Retrieval of Interacting Genes/Proteins) database version 10.0 http://string-db.org/ (Szklarczyk et al., 2015). The active interactive partners were chosen on the basis of their high confidence values based on several parameters *perse.,*co-expression, co-occurrence, neighbour, gene fusion, text-mining and experiments.The confidence score was analysed by using interaction from both shell of interactors with medium value of confidence (0.40). Structural annotation of the modelled DREB 1 protein was done using CATH server http://www.cathdb.info/ (Sillitoe et al., 2015) and functional classification was the selected CATH super-families were done using FunFHMMERhttp://www.cathdb.info/search/by-funfhmmer (Das et al., 2016) which were further analysed on basis of gene ontological (GO) terms. The identified GO terms were further analysed by using hypergeometric distribution test analysis of REVIGO web server http://revigo.irb.hr/ (Supek et al., 2011). The identification of probable subcellular localization of the selected functional GO terms was made by fetching the GO terms to CELLO2GO web server http://cello.life.nctu.edu.tw/cello2go/ (Yu et al., 2014).

2.13. Active site prediction

The predicted protein model *viz.,* DREB 1 was further analysed by using metapocket server http://metapocket.eml.org (Huang, 2009) for the prediction of the most probable ligand binding site and identification of the potential residues involved in the making of the active site.

2.14. Statistical analysis

The data of physiological and biochemical analysis were subjected to two-way analyses of variance (two-way ANOVA) with genotype and

environment as two fixed factors and means were compared by using Duncan Multiple Range Test (DMRT) at a threshold value of 0.05 with statistical software package SPSS 21.0 (SPSS Inc, Chicago, IL, USA).

3. Results

3.1. Effect of salt stress on RWC and photosynthetic pigments content

Salt stress (400 mM) substantiallyaffected RWC by 7.9–17.9% respectively in all the hybrids/parents compared to their non-stressed counterparts. Among hybrids, VRTH-1747 and VRTH-1755showed better water holding capacity as they exhibited minimum decrease (2.1–3.1%) in RWC under salt stressin contrast to control condition (Table 1).Whereas, the interactive effect of G × E on RWC was non-significant for the hybrids.The exposure of plant to salt stress at 400 mM indubitably affected chlorophyll and carotenoid contents by 62.2% and 79.5% in all the hybrids/parents under salt stress (Table 1). Hybrids, *viz.,*VRTH-1754 and VRTH-1755 showed higher chlorophyll and carotenoid contentsas compared to other hybrids under control and salt stress conditions. Significant interactive effect of G × E was observed on chlorophyll and carotenoid contents for all the hybrids.

3.2. Effect of salt stress on membrane integrity

Salt stress significantly affected membrane damage in all the hybrids which was evident by the increase in electrolytic leakage and lipid peroxidation (Table 1). Maximum damage to the membrane integrity both in terms of electrolytic leakage (5.0–15.0%) and lipid peroxidation (42.1–45.6%) was observed for the hybrids VRTH-1747 and VRTH 1749 (Table 1). However, the hybrids *viz.,* VRTH 1754 and VRTH 1755 alleviated the salt induced membrane damage showing minimum electrolytic leakage (2.2–7.8%) and lipid peroxidation (36.6%). Significant interactive effect of G × E was detected on EL and LPO for all the hybrids.

3.3. Effect of salt stress on ROS and oxidative stress generation

Imposition of salt stress (400 mM) caused significant upsurge in the oxidative damages in all the hybrids. Proline content decreased positively by 49.4–193.6% whereas H_2O_2 generationincreased significantly by 39.1–60.1% (Table 1). The hybrids *viz.,* VRTH 1755 and VRTH 1754 showed increased proline and H_2O_2 contents under salt stress compared to their respective controls. The activity of catalase (CAT) increased significantly due to effect of salt stress in all the hybrids as well in the parents. Upon salt exposure, the activity increased by 47.7–62.2% recording highest for VRTH 1754 and VRTH 1755 compared with controls, respective counterparts and parents (Table 1). The interactive effect of G × E on proline, H_2O_2 and catalase was found significant for all the hybrids as well as the parents.

3.4. Effect of salt stress on yield and related components

The tomato plants exposed to salt stress (400 mM) exhibited significantly higher reduction of 9.1–19.5%, 11.4–19.5%, 2.02–18.6% and 41.6–130.1% in fruit length, fruit width, locule number and yield/plant respectively except for total suspended solids (TSS) which showed sharp increase of 16.7–28.2% compared to their respective controls (Table 2). The hybrids *viz.,* VRTH 1755 and VRTH 1754 showed better and improved fruit length (19.8 and 6.01%), fruit width (20.4 and 17.8%), TSS (17.5 and 4.59%) and total yield per plant (45.8 and 39.2%) compared to their respective counterparts under salt stress. The interactive effect of G × E was significant for fruit length and yield and non-significant for fruit width, locule number and TSS for all the hybrids.

3.5. Effect of salt stress on expressions of defence related genes

Several stress responsive have critical functions in plant's salt stress tolerance. The genes *viz.,* ATP, DREB1, DREB2, DREB3, HSP, ZFP, LEA and EF were chosen on the basis of their putative role in transcription, protein metabolism and defence signalling response to validate changes in the expression pattern among all the tomato hybrids. Transcript abundance analysis of all the genes indicated differential response under salt stress (Fig. 1). The expression of the transcript encoding a putative DREB transcription factors *viz.,* DREB 1 (75 and 79,6%), DREB 2 (74 and 69.8%) and DREB 3 (77.4 and 74.0%) were significantly increased in VRTH 1755 and VRTH 1754 hybrids compared to their respective counterparts and parents upon salt exposure (Fig. 1). Similarly, the relative abundance of ATP (82.4 and 78.9%), HSP (56.4 and 52.8%) and ZFP (71.4 and 65.8%) were also found to be upregulated in both VRTH 1755 and VRTH 1754 hybrids and were downregulated in VRTH 1747 and VRTH 1749 hybrids and parents.The expression of LEA (62.3 and 69.4%) and EF (42.3 and 62.6%)showed differentialresponse under salt stress as their expression was repressed in VRTH 1747 and VRTH 1749 hybrids. However, both LEA (78.4, 70.5 and 50%) and EF (67.0, 59.4 and 50%) were induced upon salt exposure in VRTH 1755, VRTH 1754 and KT-8. Overall, the results confirmed that the expression of all the selected genes were significantly upregulated in VRTH 1755 and VRTH 1754 hybrids compared to VRTH 1747 and VRTH 1749 (Fig. 1).

3.6. Database search and comparative phylogeny

The BLAST-P search against non-redundant (nr) database reveal all the possible homologs for dehydration responsive element binding (DREB 1) protein 1 in tomato. Sequences showing extreme identity (100%) acquiring maximum query coverages (100%) with the target sequence were exploited for further study. The phylogenetic tree based on maximum likelihood methods revealed monophyletic origin and relatedness of SlDREB1 (NP_001234689.1)with its wild homologue *Solanum pimpinellifolium* (AKC42089.1) and close resemblance with *Solanum pennelli* (XP_006353419.1) than *Solanum tuberosum* (XP_006353419.1) (Fig. 2A). On the contrary, the other members of the family *viz.,Capsicum annum* (XP_016573418.1) and *Nioctiana tabacum* (XP_016461559.1) formed a separate out-group (Fig. 2A). The result clearly indicated that SlDREB1 was of recently evolved compared to other homologous/orthologous members of tomato family. The multiple sequence alignment of functional domain from DREB1 protein sequences showed maximum conservation of amino acid residues in the entire stretch of protein among all the members (Fig. 2B). Strongest conservation of core amino acid residues around KYRG domain regionmight be the crucial sites for binding of DREB1 proteins to the DRE elements as minimal disturbanceshad occurred during the course of their phylogenetic evolution.The similarities and the differences among different tomato members and with the other homologs and orthologs was also compared by using circos visualization tool. At 50% cut-off values, the SlDREB1 showed no relation with *Nicotiana tabacum*.However, SlDREB1 showed strong relationship with *Solanum pimpinellifolium* and *Solanum pennelli*whereas least was observed with *Solanum tuberosum* and *Capsicum annum* (Fig. 3).The intensity of the circos colour bands indicate the level of conservation of amino acid residues across the relevant members.

3.7. Distribution of conserved motifs

The distribution of the functionally conserved network elements (motifs) with in the tomato family were scanned by subjecting complete DREB1 protein sequences of tomato to Multiple EM (Expectation Maximization) for Motif Elicitation (MEME) analysis tool. In total, 19 conserved motifs were identified which showed strong conservation of AP2 domain across all the members for DREB1 protein (Fig. 4A). The

Table 2
Changes in yield and related attributes in tomato hybrids/parents subjected to 400 mM of salt stress.

Hybrids/parents	Treatments	GH	FS	FL (cm)	FW (cm)	LN	TSS	Y/P (Kg/plant)
VRTH-17-55	Control	Determinate	Oval round	5.10 + 0.15^{a}	6.26 + 0.19^{a}	5.07 + 0.34^{ab}	4.70 + 0.21^{bc}	12.0 + 0.41^{a}
	400 mM			4.68 + 0.23^{a}	5.39 + 0.22^{a}	4.55 + 0.17^{ab}	6.55 + 0.26^{a}	8.47 + 0.24^{a}
VRTH-17-47	Control	Indeterminate	Oval round	4.80 + 0.15^{b}	5.94 + 0.12^{b}	4.53 + 0.26^{bc}	4.47 + 0.18^{bc}	11.0 + 0.28^{cd}
	400 mM			4.11 + 0.17^{b}	5.23 + 0.14^{a}	4.42 + 0.20^{ab}	5.77 + 0.25^{b}	5.60 + 0.24^{d}
VRTH-17-54	Control	Determinate	Oval round	4.77 + 0.11^{b}	5.82 + 0.18^{b}	4.43 + 0.28^{c}	4.50 + 0.24^{bc}	11.8 + 0.32^{bc}
	400 mM			3.99 + 0.16^{bc}	5.22 + 0.16^{a}	4.30 + 0.22^{b}	5.66 + 0.21^{b}	7.56 + 0.25^{b}
VRTH-17-49	Control	Determinate	Round	5.00 + 0.15^{a}	5.82 + 0.23^{b}	4.27 + 0.16^{c}	4.77 + 0.24^{b}	13.0 + 0.35^{a}
	400 mM			4.04 + 0.20^{bc}	5.15 + 0.17^{a}	4.34 + 0.19^{b}	5.73 + 0.30^{b}	5.63 + 0.28^{d}
KT-8 (Salt tolerant)	Control	Semi indeterminate	Round	4.70 + 0.15^{b}	5.87 + 0.14^{b}	5.50 + 0.24^{a}	5.40 + 0.15^{a}	10.4 + 0.33^{d}
	400 mM			4.10 + 0.17^{b}	5.14 + 0.13^{a}	4.76 + 0.27^{a}	6.65 + 0.17^{a}	6.71 + 023^{c}
Agata-30 (Salt enduring)	Control	Determinate		4.33 + 0.18^{c}	5.13 + 0.14^{c}	4.39 + 0.19^{c}	4.34 + 0.18^{c}	9.30 + 0.35^{e}
	400 mM			3.75 + 0.21^{c}	4.29 + 0.19^{b}	3.70 + 0.19^{c}	5.53 + 0.18^{b}	4.59 + 0.22^{e}
Two-Way Anova								
Genotype				***	***	***	***	***
Environment				***	***	***	***	***
Genotype × Environment				*	NS	NS	NS	***

The values of GH: Growth habit, FS: Fruit shape, FL: Fruit length, FW: Fruit width, LN: Locule number, Y/P: Yield/plant (means of three replicates ± SE) in the same column with different letters are significantly different at the 0.05 level according to Duncan's multiple range test from each other ($P < 0.05$). Data were analysed with two-way ANOVA. *$P < 0.05$; **$P < 0.01$; ***$P < 0.001$; NS; not significant.

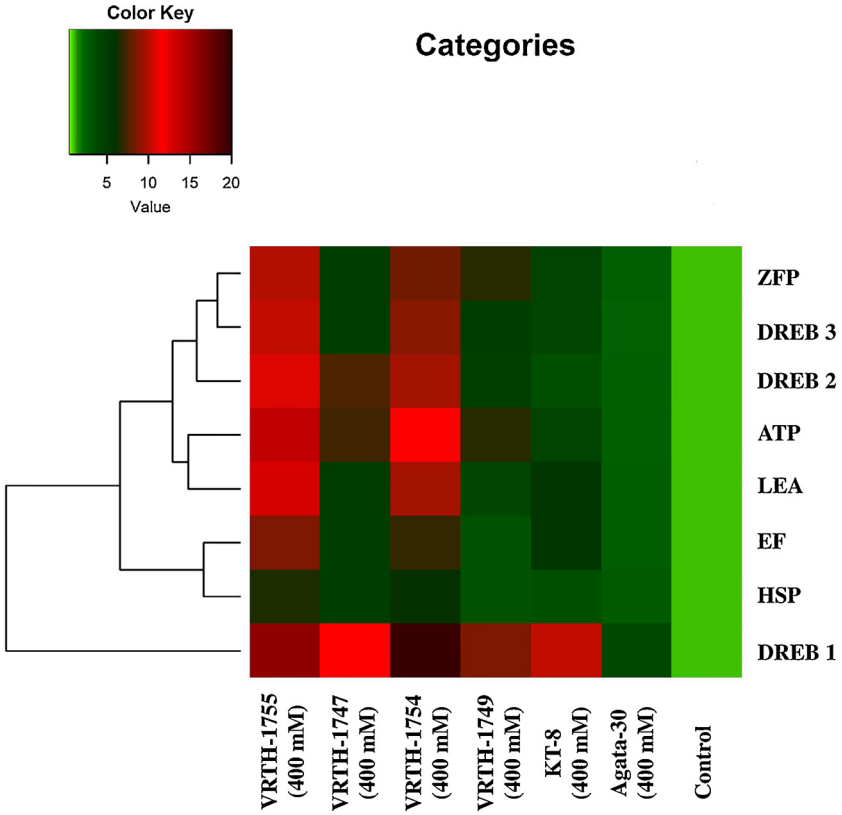

Fig. 1. Heat Map and clustering analysis of stress responsive genes in hybrids and parents of *S. lycopersicum*under salt stress (400 mM).

distribution of motifs was also analysed in the form of phylogenetic tree that also clustered *S. lycopersicum, S. pimpenellifolium* and *S. pennelli* into one group with *S. tuberosum* evolutionary closer to above three compared to *C. annum* and *N. tabacum* (Fig. 4A). The significance of motifs wasevaluated in statistical terms of their *E*-value which is a conservative value that provides frequency of occurrence for each motif whereas the *p*-value denotes the probability of their occurrence. In our results, the N-terminal domain (NTD) from SlDREB1 was represented by motif 7 (MAIMDQAANM; *p*-value 8.0e -16), AP2 domain (Fig. 4B) was constituted by motif 1 (YRGVRQRIWGKWVAEIREPKRGSRLWLGTF; *p*-value 2.3e – 39) whereas C terminal domain was represented by motif 4 (MDIVEPTSIDEDTLKSGWDCLDKLNMDEMF; *p*-value 9.1e – 40). The motif scanned by MEME and MAST analysis reveal that functional motifs depicting N-terminal, C-terminal and AP2 domains were strongly conserved among all members of tomato family.

The result of motif scan analysis is in the conformity of the results of the multiple sequence alignment done for the full length SlDREB1 protein revealing the conservation of core residues which was also clearly reflected from our motif distribution analysis. However, presenceof certain conserved motifs among different DREB1 family member provide an estimate of unique motifs for certain group. Therefore, in the present study, absence of fifth and seventh motifs and

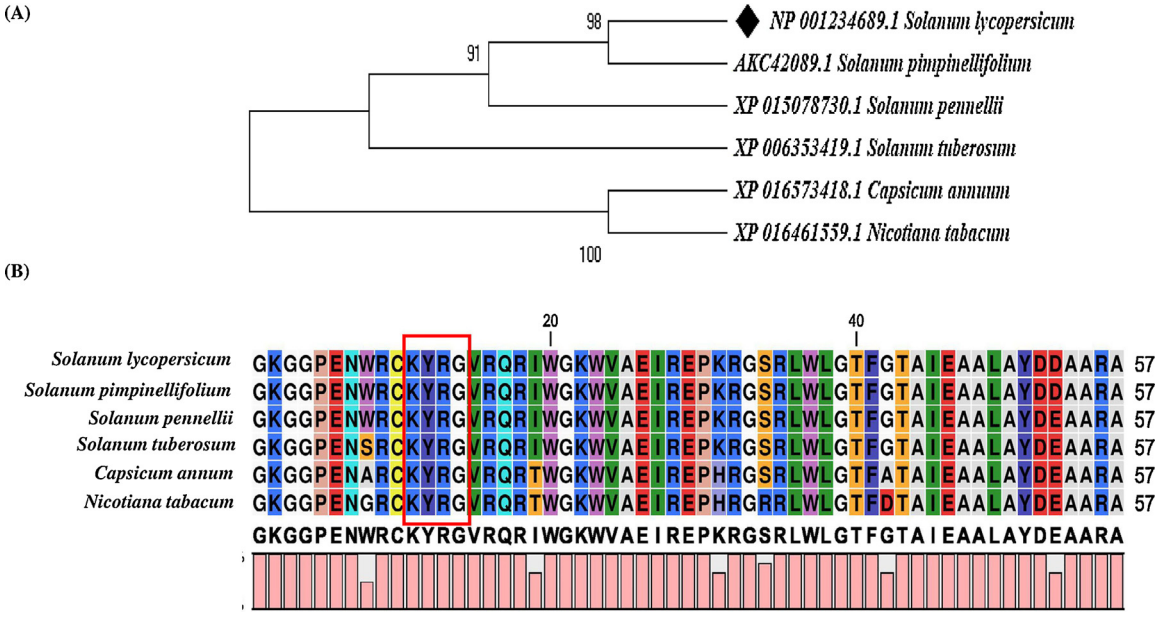

Fig. 2. Phylogenetic tree showing (A) evolutionary relationship and emergence (B) sequence alignment of the conserved functional domain of *Solanum lycopersicum* dehydration responsive element binding (SlDREB1) protein among different members of solanaceous family.

presence of additional two motifs *viz.,*motif 12 (PMTNDPGFDF; *p*-value 1.6e – 11) and motif 13 (DNNFVSDDQCF; *p*-value 5.5e – 12) was observed in *S. pimpenellifolium*signifies the sequence divergence with in the same group (Fig. 4A). Similarly, motif 10 (LPTVSQSGSNT; *p*-value 1.6e – 11) and motif 11 (IKEEPIAFEY; *p*-value 1.7e – 12) were found to be present in both *C. annum* and *N. tabacum* but absent from *S. lycopersicum, S. pimpenellifolium* and *S. pennelli*indicating their common phylogenetic origin and their subsequent divergence from *C. annum* and

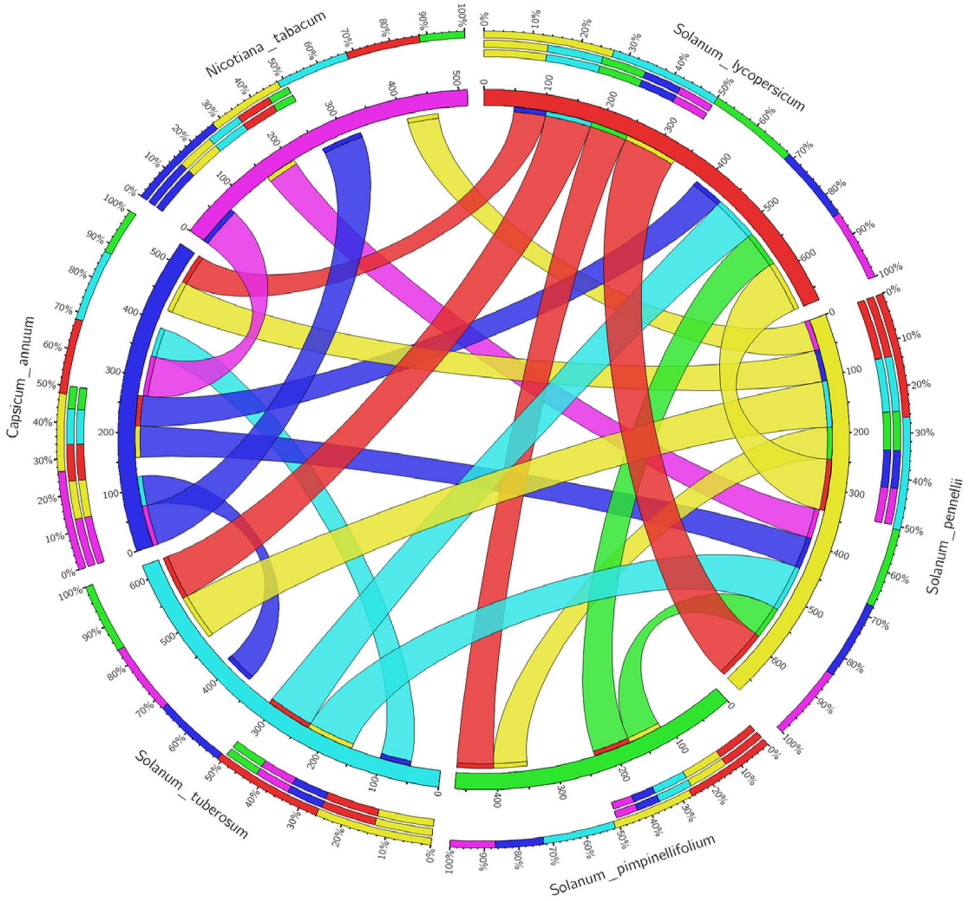

Fig. 3. Comparative analysis of similarities and differences in *Solanum lycopersicum* dehydration responsive element binding (SlDREB1) protein among different members of solanaceous family.

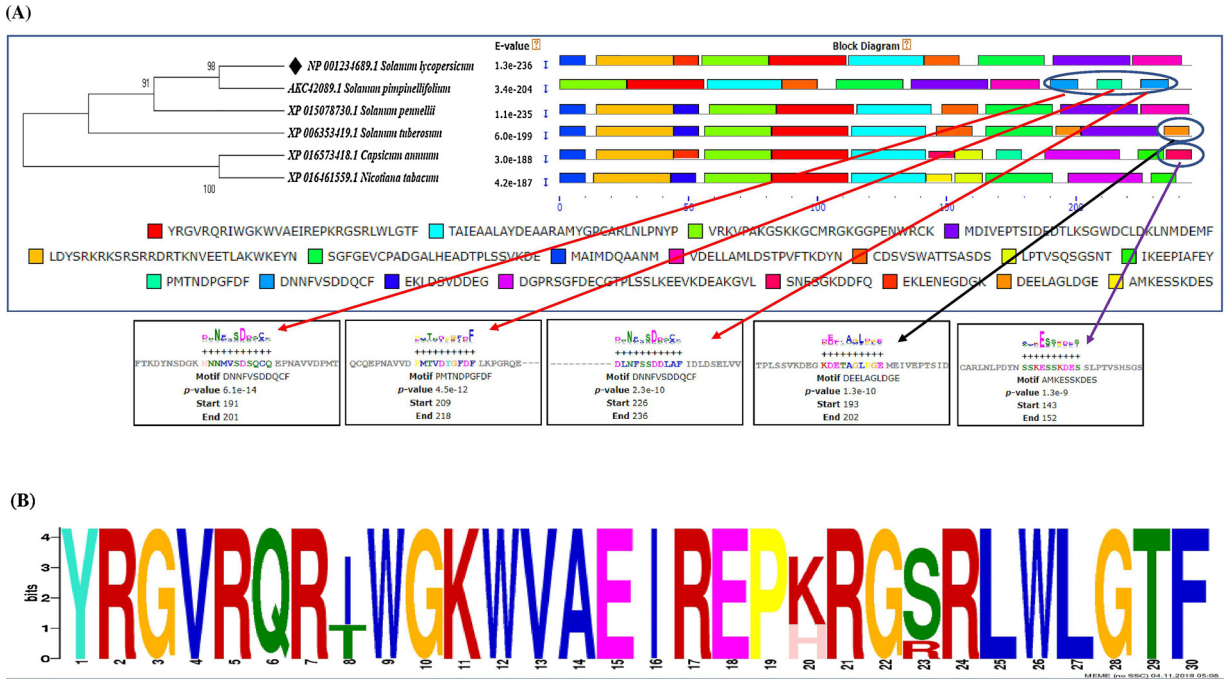

Fig. 4. The motif scan analysis showing distribution and presence /absence of common and uncommon motifs found in *S.lycopersicum, S. pimpenellifolium, S. pennelli, S. tuberosum, C. annum and N. tabacum* discovered through MEME and MAST analysis. **(A)** The block diagram showing the sequence of discovered motifs for SlDREB1. The red arrows indicate the presence of uncommon motif in *S. pimpenellifolium,* black arrows indicate the presence of uncommon motifs in *S. tuberosum*and purple arrows indicate presence of uncommon motifs in *C. annum*which are absent in other members. **(B)** The sequential logo of the motif 1 showing consensus sequences present in all the representatives' members.

N. tabacum from the same family (Fig. 4A). Furthermore, presence of additional motif 16 (SENESGKDDFQ; *p*-value 3.0e – 11) in *N. tabacum* which was absent in all the other members may provoked *N. tabacum* to form separate cluster. The motif logo diagram for motif 1 having KYRG sequences lying in the AP2 DNA binding domain showing highest conservation among all the members as indicated by the height of the alphabetical letters have been depicted in Fig. 4B.

3.8. Gene prediction and whole genome sequence analysis

For gene prediction and whole genome shortgun sequence analysis SlDREB1 protein sequence was subjected to TBLASTN analysis. The TBLASTN analysis predicted the probable whole genome shortgun sequences available across tomato genomes*viz.,*BABP01006590.1 (Identity 84%; Query cover 100%), AEKE03003142.1 (Identity 84%; Query cover 100%), AEKE03003141.1 (Identity 37%; Query cover 98%), BABP01092002.1 (Identity 45%; Query cover 43%) (Supporting information Figure S4).The first hit BABP01006590.1 (with identity 84% and query cover 100%) was further subjected to gene prediction analysis through fgenesh gene prediction tool that significantly predicted coding sequences, transcriptional start sites (TSS), Poly A tail along with the probable protein sequences which were in accordance with the input nucleotide sequences for SlDREB1 (Fig. 5). Further, the first hit (BABP01006590.1) obtained after TBLASTN analysis was subjected to BLAST-P analysis of uniprotKBdatabase to identify putative homologs/orthologs for the input query SlDREB1 protein. The uniprotKB BLAST-P analysis of query protein showed 100% homology with DREB protein of *S. lycopersicum* (Q8GZF2) and with *S. pimpinellifoilum* (Supporting information Figure S3) thus revealing close evolutionary relationships between *S. lycopersicum* (Q8GZF2) and *S. pimpinellifoilum*for thequery protein as confirmed by phylogenetic tree constructed based on protein BLAST annotations and circos plot. **Identification of functional domain and sites**

Identification of functional sites underlying the SlDREB1 protein sequence was done by submitting sequence to ExPASy PROSITE online tool (http://prosite.expasy.org). The results of PROSITE scan retrieved the functional signature sequence at N-terminal end that constitute KYRG (AP2/ERF) domain region occupying in the protein and also confirmed that the SlDREB1 protein belong to AP2/ERF gene superfamily. Furthermore, InteProScan scan analysis also revealed the presence of KYRG (AP2/ERF) DNA binding domain that span from 1- 140 amino acid residues in which the core signature sequences cease to exist between Lys^{81} and Pro^{138} (Supporting information Figure S5). The propensity of the signature sequences obtained for SlDREB1 after PROSITE analysis was further confirmed by multiple sequence alignment done for the functional domain region *viz.,* KYRG (AP2/ERF) (˜60 amino acids) showed strong conservation of the core signature sequences across all the members.

3.9. Structural modelling and superimposition of KYRG domain

The N-terminal DNA binding domain of SlDREB1 was modelled using appropriate templates chosen on the basis of sequence similarity and residue completeness. DS Modeller generated a total of five models for SlDREB1 (Table 3) and the model with least RMSD (Cα trace) value with respect to crystal structure of template was selected for further interactions. In the present result, the modelled N-terminal domain for SlDREB1 (Fig. 6A) was good in terms of total calculated electrostatic energy (minimum) which is an important parameterthat depict stability and reliability of protein structures (Pokala and Handel 2005). The specifically recognized GCC box sequence (DRE elements; 5′-TACCGA CAT-3′) (Fig. 6B) for DNA-protein interaction studies was modelled using DNA sequence to structure tool (http://www.scfbio-iitd.res.in/software/drugdesign/bdna.jsp) (Arnott et al. 1976). The predicted model with good score values was submitted to PMDB that assigned PMDB ID (PM0091904) for our submitted structure (Supporting information Figure S6).Structural resemblance of different proteins structures despite of sequence similarity and divergent evolution has been well documented. Therefore, the predicted SlDREB1 model was superimposed on each template to assess their topological details

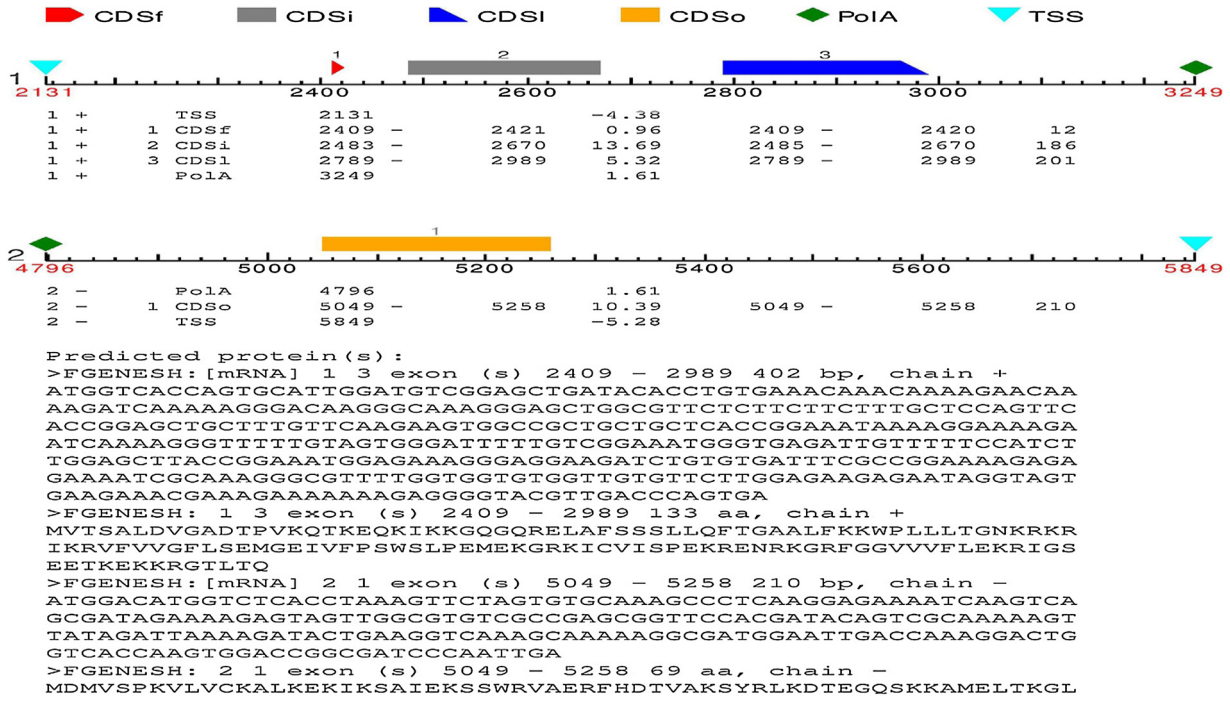

Fig. 5. Whole genome sequence and gene prediction analysis in SlDREB1 using TBLASTN and Fgenesh (HMM based gene prediction) tools for identification of transcriptional start sites and Poly A sequences.

Table 3
Molecular PDF energy, GA341 score and DOPE score for modelled SlDREB1.

Model name	Molecular PDF energy	GA341 score	DOPE score
Predicted model scores for DREB1			
MODEL 1 (B0001)	286.6218	1.00000	− 4311.87695
MODEL 2 (B0002)	323.5970	0.99999	− 4259.92139
MODEL 3 (B0003)	349.9475	0.99999	− 4225.76904
MODEL 4 (B0004)	364.0876	0.99998	− 4234.29150
MODEL 5 (B0005)	333.5226	0.99997	− 4339.36377

(Fig. 7). The superimposition results from SALIGN web server showed high similarity between the target protein (SlDREB1) with its template structures. The structural alignment for predicted model showed high similarity with 1GCC, 2GCC and 3GCC templates as compared 5WX9 which was further confirmed by observed local and global RMSD values for each template. The RMSD values when the predicted model was superimposed on 1GCC, 2GCC, 3GCC were 1.00 Aº, 0.80 Aº, 0.57 Aº alpha carbon and 1.01 Aº, 0.83 Aº, 0.65 Aº around the backbone confirming that the AP2/ERF domain structures are highly conserved with high level of sequence similarity across the divergent AP2/ERF members (Fig. 7A, B, C). Whereas, when SlDREB1 was superimposed over template 5WX9 the calculated RMSD values were found to be 1.77 Aº alpha carbon and 1.75 Aº around the backbone which unveil synonymous or non-synonymous substitutions of some amino acid residues thereby distinguishing 5WX9 templates from rest of template structures and predicted protein (Fig. 7D).

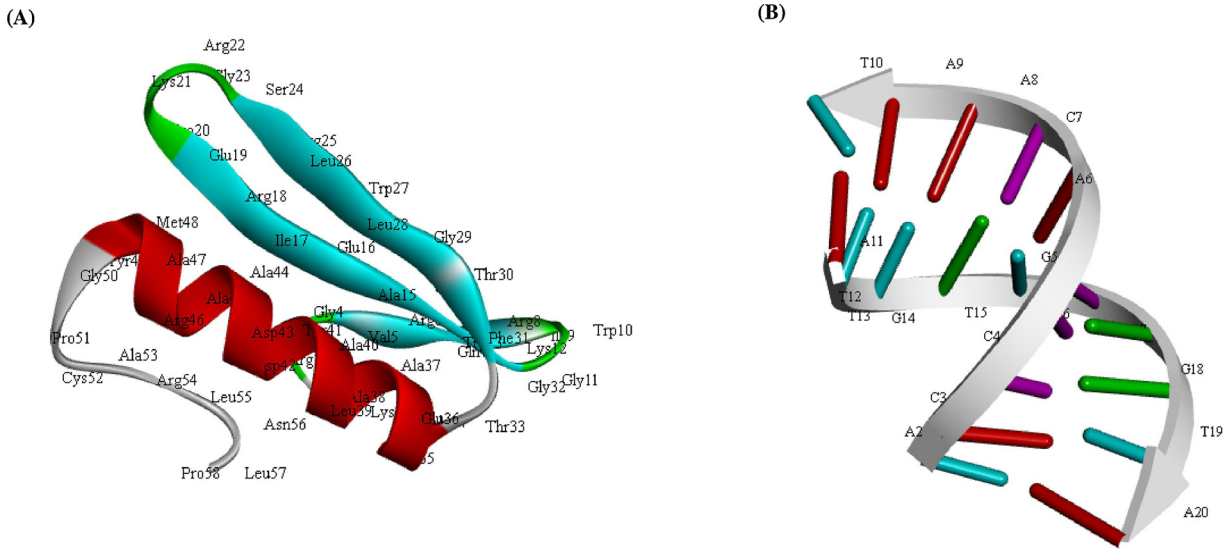

Fig. 6. Predicted structures of **(A)** functional domain of SlDREB1 generated by MODELLER module of Discovery Studio 3.0 **(B)** structure of the dehydration responsive element (DRE) (TACCGACAT).

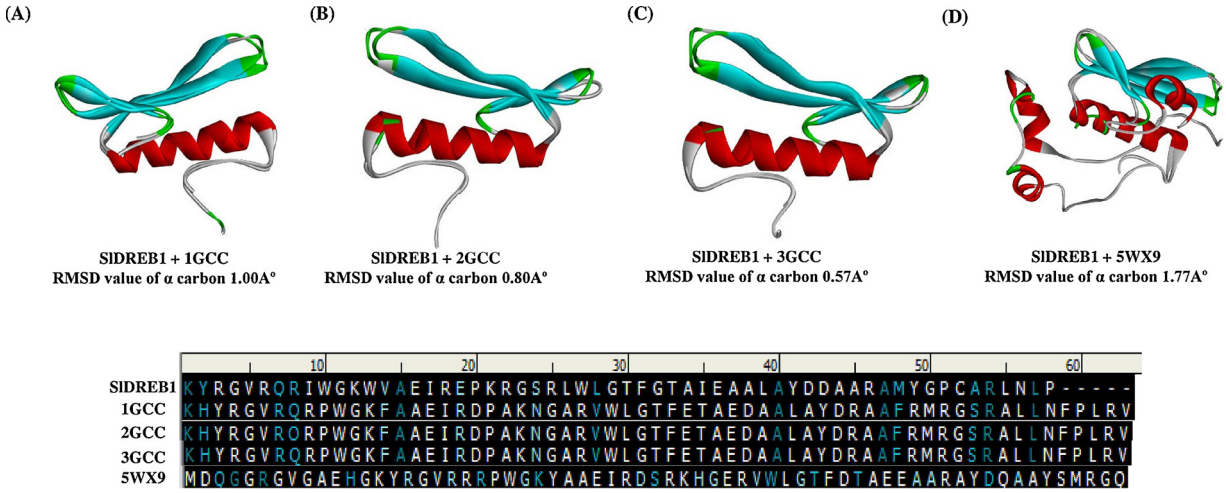

Fig. 7. Superimposition results represented with their respective global and local RMSD-values showing the structural conservation of SlDREB1 domain. Sequence alignment between SlDREB1 with the respective templates (1GCC, 2GCC, 3GCC and 5WX9) predicts the synonymous (blue) and non-synonymous substitutions (white).

3.10. Model evaluation and validation

The three-dimensional (3D) model of SlDREB1 was generated using Modeller Discovery Studio Client 3.0 by aligning and satisfying all the spatial parameters in terms of probability density functions (PDFs) and discrete optimized protein energy (DOPE) which statistically assessed the homology of the modelled protein. The DS modeller generated a total of five models which were arranged on the basis of essential energy and stability parameters. The model with the lowest DOPE and GA341 score was selected for DNA-protein interaction study (Table 3). The qualitative assessment of our predicted model (SlDREB1) was performed using Ramachandran plot analysis using RAMPAGE server and PROCHECK analysis using PDBSum server concluded that 100% of the amino acid residues were observed in most favoured regions against ˜98% expected value and 0.0% residues were detected in allowed regions against ˜2.0% expected value (Table 4). The results obtained from RAMPAGE server was also confirmed by the results of PROCHECK analysis of PDBSum server which also predicted that 100% of the residues occurred in the most favoured region (A,B,L), 0.0% residues were observed in additional allowed regions (a, b, l, p) and no residues were found in the disallowed regions as compared to respective templates (Fig. 8A).

Furthermore, the results of ProSA server also validated that the predicted model (SlDREB1) has minimum structural error difference in terms of Z score and was very close to the NMR resolutedtarget template proteins (Table 4; Fig. 8B). The ERRAT analysis of modelled protein exhibited an ERRAT score of 94.0% which also confirmed that the atomic bonding interactions with in the predicted model was good as compared to respective templates (Table 4). The superiority of our computed model was also validated by Resolution by Proxy (RESPROX) analysis which also authenticated that the predicted model (SlDREB1) had better atomic resolution than template proteins (Table 4). Additionally, the predicted model was subjected to Qualitative Model Energy Analysis (QMEAN) for the assessment of geometrical aspects in terms of long-range interaction which also confirmed the predicted model was of good quality as compared to respective experimental structures (Table 4). The quantitative aspects of the modelled protein were confirmed by VADAR results that evaluated the model for its stereo quality index, fractional accessible surface area, functional residual volume and other quantitative statistics. The VADAR results predicted that computed model (SlDREB1) existed as coiled type structure 22 (37%), beta 20 (34%) and 16 (27%) helix type configuration with the observed H bond energy (-2.1, SD = 1.1) against expected (-2.0, SD = 0.8).

3.11. DNA-protein interaction

The most reliable model (SlDREB1; Fig. 6A) satisfying all the qualitative and quantitative energy parameters were docked with the specially recognised 3D structure of GCC (DRE element; Fig. 6B) box sequence for the identification of core amino acid residues involved in the interaction with the ligand (GCC box DNA element) and the binding energy for most stable complex was calculated. In our result, the most stable docked complex has binding energy (E_{total} = -537.64 Kcal/mol) which confirm the stability of the docked complex as substantiated by low energy (most negative) of the docked complex (Supporting information Figure S7). The DNA-protein interaction studies revealed that SlDREB1 binds with GCC-box DNA sequence through conserved KYRG motifs (Fig.9A). The key residues which were involved in the interaction were Arg^{18}, Glu^{19}, Pro^{20}, Lys^{21}, Arg^{22}, Leu^{26}, Trp^{27}, Leu^{28}, Asp^{43}, Ala^{44}, Arg^{46}, Ala^{47}, Met^{48}, Tyr^{49}, Gly^{50}, Pro^{51}, Cys^{52}, and Arg^{54}(Fig. 9A; 9B) as compared to NMR derived solution structure of AtDREB1 (1GCC) in which the interacting residues was also conserved YRG motifs comprising Gly^{148}, Val^{149}, Arg^{150}, $Arg^{15}2$, Trp^{154}, Lys^{156}, Glu^{160}, Ile^{161}, Arg^{162}, Pro^{164}, Gly^{168}, Arg^{170}, Trp^{172}, Gly^{174}, Thr^{175} and Tyr^{186}thereby confirming that similar consensus core residues of KYRG motifs are involved in binding as those found in AtDREB1 (Fig. 9A).

3.12. Protein-protein interaction

The assessment of functional interactive network made by SlDREB1 was analysed by the results obtained by STRING server at medium confidence level by selecting default custom values of 10 interactors form both first shell and second shell (Fig. 10). At medium confidence interval, we observed that SlDREB1 (Solyc06g050520.1.1) was found to be in interaction with only one protein *viz.,*diphthine ammonia ligase enzyme (Solyc04g010080.2.1; score value 0.901) from its first shell of interactors, which is an uncharacterized protein with possible role as eukaryotic elongation associated factor. Whereas the SlDREB1 (Solyc06g050520.1.1) was found to have interaction with several proteins from second shell interactors displaying maximum score values of 0.913 and 0.878 with an uncharacterized protein (Solyc08g062910.2.1 andSolyc12g062900.1.1) having translation elongation factor activity and GTPase activity and lastly with ubiquitin binding like protein (Solyc04g079840.2.1 and Solyc05g052910.2.1; score value 0.901) which are involved in metal ion binding (Fig. 10). The results of the present study have shown all the possible interactive partners associated with SlDREB1 protein (Supporting information Table S2) which eventually confirm the involvement of the DREB1 protein in different

Table 4
Assessment of qualitative and quantitative scores for the modelled DREB1 protein and its comparison with the experimentally deduced (X-ray diffracted/NMR) structures.

S. No	Protein name	Qmean score	Z score	Overall quality Errat score	ReSProx	Rampage results			
						Most favoured (%)	Additionally allowed (%)	Outlier region (%)	
1.	SlDREB1 dehydration responsive element binding protein 1 *S. lycopersicum* (NCBI ID: NP_001234689.1) (predicted model)	0.02	−3.60	94.00	1.39	100	0.0	0.0	
2.	Complex of GCC-box binding domain of ATERF1 and GCC-box DNA (PDB ID: 1GCC) (Template 1)	−0.17	−3.83	94.44	1.25	95.1	4.9	0.0	
3.	GCC-box binding domain, NMR, minimized mean structure (PDB ID: 2GCC) (Template 2)	−1.87	−3.91	53.84	2.77	85.2	11.5	3.3	
4.	Solution structure of the GCC-box binding domain (PDB ID: 3GCC) (Template 3)	−1.68	−3.76	43.63	2.70	88.5	8.2	3.3	
5.	Crystal Structure of AtERF96 with GCC-box (PDB ID: 5WX9) (Template 4)	−5.58	−2.89	50.86	3.04	93.2	3.9	3.9	

A good quality protein have ReSProx values ranging between 0–1.5, Errat score more than 90, minimum Z and Qmean scores with occupying more than 98% of the residues in most favoured region, less than 2% residues in additionally allowed region and 0% residues in outlier region in RAMPAGE analysis.

signalling pathways thus revealing their mode of function and regulation across different AP2/ERF members.

3.13. Gene ontology (GO) enrichment analysis

The SlDREB1 protein sequences were further analysed by CATH and Gene3D server to predict their role in biological processes, molecular function and its subcellular localization. The ReviGO analysis characterized all the significant GO terms through simple clustering algorithm and made visualized them in scatter plot diagram that represent their functional values in the form of unique colours. In the present study, five significant GO terms under biological process were positive regulation of transcription (GO: 0045893), ethylene activated signalling pathway (GO: 0009873), response to cold (GO: 0009409), response to water deprivation (GO: 0009414) and response to salt stress (GO: 0009651) (Fig. 11A). Whereas, the significant GO terms under molecular function were transcription factor activity (GO: 0003700), sequence specific DNA binding (GO: 0043565), protein binding (GO: 0005515), transcriptional repressor activity (GO: 0001078) and identical protein binding (GO: 0042802) (Fig. 11B). In addition, the Cello2GO results predicted the most significant subcellular localization of SlDREB1 protein to the chloroplast (32.9%; score value 1.64) mostly involved in the biological function such as ethylene mediated signalling pathway, transcription initiation and defence response. Whereas, 28.9% of the SlDREB1 protein belongs to nucleus (score value 1.44) performing sequence specific DNA binding transcription factor activity and 17.6% of the SlDREB1 protein were localised in cytoplasm (score value 0.881). The cellular component revealed that the predicted protein probablyis an integral component of nucleus (Fig. 12).

4. Discussion

Plants contrive salinity tolerance through adaptation or acclimation process by improvising at physiological, biochemical and molecular levels to prevent the disruption of ions/osmotic homeostasis, thus impeding water loss and expediting photosynthetic process (Shabala and Munns, 2017). The sensitivity of plants to salt stress depends upon the intensity of the stress and associated factors, plant species and their developmental stages (Anjum et al., 2011). Our results demonstrated differential response of four tomato hybrids along with salt-tolerant/salt-susceptible parents and evaluated the degree of their tolerance. RWC was observed higher for VRTH-1754 and VRTH-1755 hybrids compared to other hybrids/parents thereby asserting their competency in retaining water under salt stress. Increased leaf relative water potential in these hybrids may be due to the increased accumulation of osmolytes proline which is widely known to permit osmotic adjustment by regulating the synthesis of other antioxidants *perse*., catalase and upregulation of Late embryogenesis abundant (LEA) proteins thus regulating ion sequestration more efficiently as compared to other hybrids (Tounekti et al., 2011). Salt stress is widely known to reduce RWC in various plants including wheat, henna and grapevine (DaCosta and huang, 2007; Fernandez-Garcia et al., 2014; Ikbal et al., 2014). All the hybrids expressing symptoms of salt stress delineated significant reduction in both chlorophyll and carotenoid contents with respect to control. This decrease in the photosynthetic efficiency in NaCl treated tomato hybrids may be due to the fact that salt stress may have provoked stomatal closure in these hybrids as an efficient adaptive transpiration control to limit water loss (Hessini et al., 2009). On the other hand, higher level of photosynthetic pigments in VRTH-1754 and VRTH-1755 hybrids might be due to increased leaf turgor by the virtue of increased ion sequestration thus decreasing energy dissipation and allowing ceaseless supply of CO_2 to RUBISCO hence causing up-regulation of photosynthesis(Munns and Gilliham, 2015; Tang et al., 2015).

Salt stress often leads to generation of reactive oxygen species which severely effect cellular membranes provoking lipid peroxidation

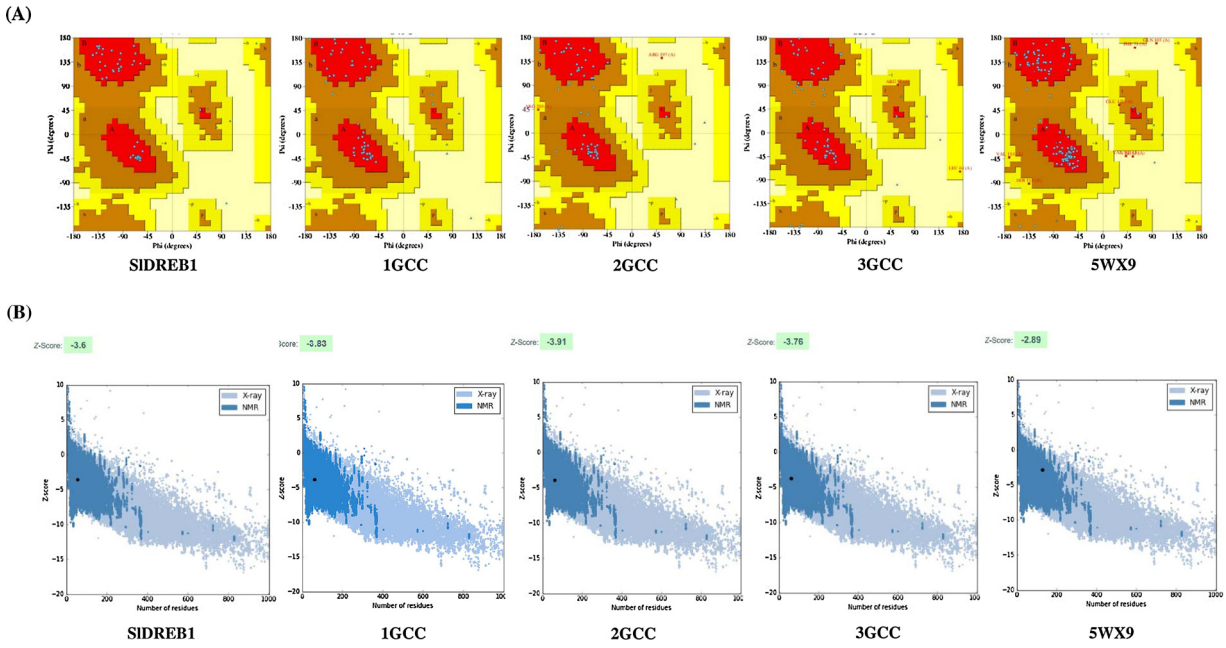

Fig. 8. Qualitative analysis of predicted model using PROCHECK and ProSA analysis. **(A)** The stereo chemical spatial arrangement of amino acid residues in predicted model (SlDREB1) were compared with experimentally resolved structures (1GCC, 2GCC, 3GCC and 5WX9) through PROCHECK server. **(B)** Qualitative estimation by ProSA server, that measures structural errors in each amino acid residues.

causing oxidative damages (Shabala and Munns, 2017). In the present study, both electrolytic leakage and lipid peroxidation was markedly increase in all NaCl treated hybrids probably due to the increased malondialdehyde and hydrogen peroxide contents. However, hybrids *viz.,* VRTH-1754 and VRTH-1755 showed minimum disruption of membrane integrity and hydrogen peroxide content. Higher membrane integrity in these hybrids might be due to the increased accumulation of heat shock proteins (HSPs) controlling protein denaturation in cell wall-plasma membrane connections as well as enhanced expression of elongation factor proteins that induces the protein synthesis upon salt exposure(Xu et al., 2008; Gomez-Bellot et al., 2013). Plants in response to salt stress and other climate extremes, accumulates osmo-protectant

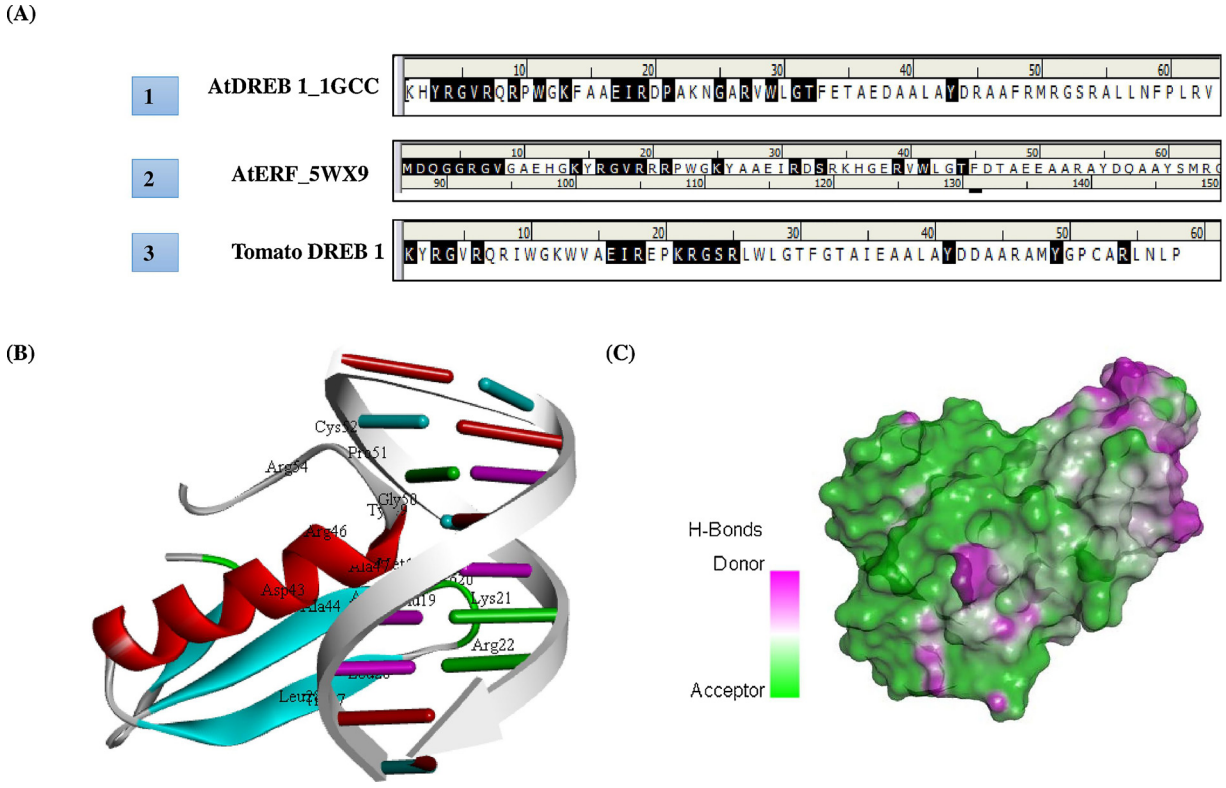

Fig. 9. A) Comparative analysis of docked complex with experimentally resolved X-RAY diffraction structures of functional domain of 1GCC and 5WX9 with DRE motif **(B)** Structure of docked complex (SlDREB1 with DRE motif) as visualized Discovery Studio 3.0 **(C)** Three-dimensional surface view for SlDREB1-DRE interaction highlighting the docked complex in terms of hydrogen bonds donor and acceptor groups in docked complex.

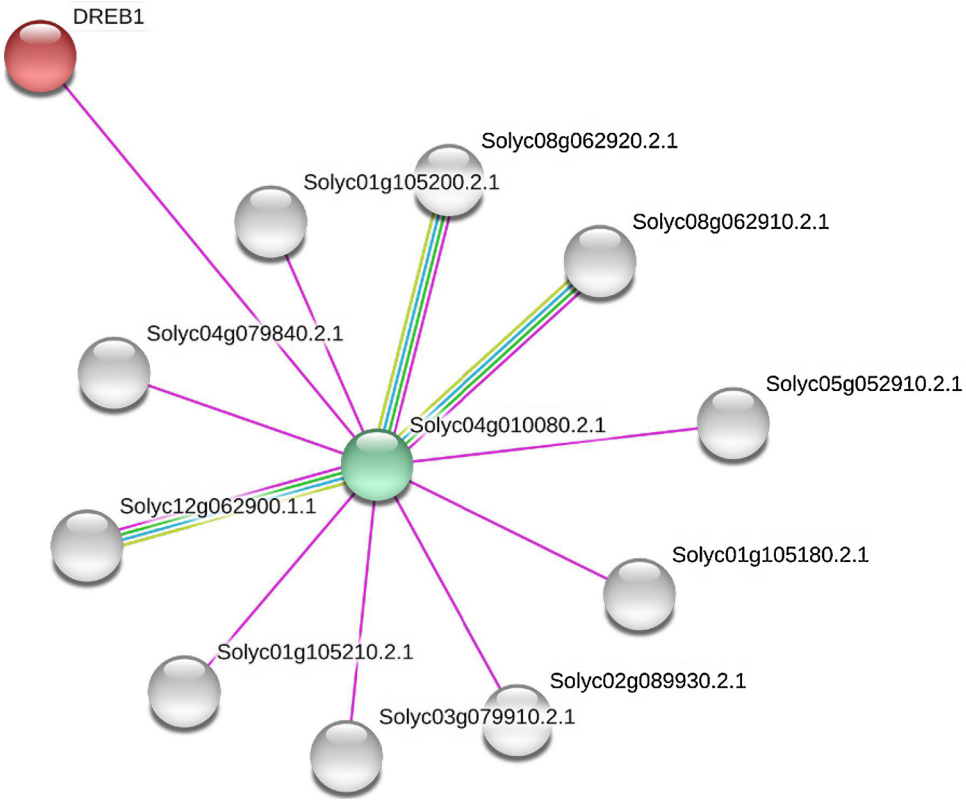

Fig. 10. Functional interactive network of SlDREB1 with other protein family members as found on STRING server where the coloured nodes describe query proteins from first shell interactors and white nodes are form second shell interactors. The large node size represents characterized proteins and smaller nodes for uncharacterized proteins.

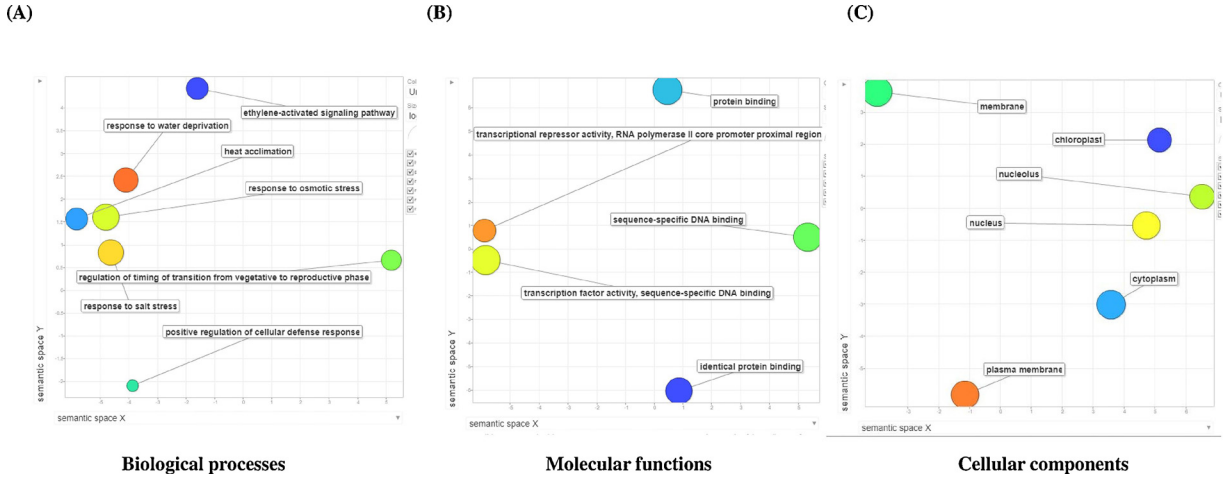

Fig. 11. Gene ontology analysis using ReviGO web server. The functional and significant GO terms involved in **(A)** biological processes and **(B)** molecular function **(C)** cellular components are shown on scattered plot diagram using hypergeometric test distribution of SlDREB1.

molecules such as proline for improving water absorption thereby adjusting ion/osmotic homeostasis (Ashraf and Foolad, 2007; Anjum et al., 2011). In the present study, the NaCl treated plants exhibited significantly higher level of proline as compared to non-stressed control plants especially in VRTH-1754 and VRTH-1755 hybrids. In the present study, enhanced expression of Zinc finger protein might be responsible for greater accumulation of free proline to combat against the stress. The enhanced expression of ZFP has been significantly reported to regulate the expression of pyrooline – 5 – carboxylatesynthetase (P5CS) which is a natural transporter of proline that improve plant growth and survival by increasing stress tolerance in many plants (Anjum et al., 2011; Nazar et al., 2011). Under stress conditions, accumulating higher level of antioxidant enzymes may contribute to salt tolerance by increasing reducing capacity against oxidative damage in plants exposed to varying abiotic stresses (Liu et al., 2011). Analogous results were observed in the present study where the activity of catalase enzyme increased significantly in all the hybrids recording highest in VRTH-1754 and VRTH-1755 compared to respective counterparts under stress and non-stress condition. Upregulation of various stress responsive genes in the present study might have caused increased accumulation of catalase activity with enhanced ROSs scavenging capacity leading to improved salt tolerance (Bian and Jiang, 2009; Bita and Gerats, 2013).

Suppression of plants yield and related traits under salt stress condition is a general phenomenon (Ashraf and Harris, 2004), whereas the suppressive effect of salt stress varies differentially depending upon plant organs and idiotypes. In this study, fruit length and yield/plant were affected more compared to fruit width, locule number and total soluble solids where the effect was observed less for VRTH-1754 and VRTH-1755 hybrids (Table 2). Photosynthesis is the process that anchor plant growth and productivity and in the present result highest

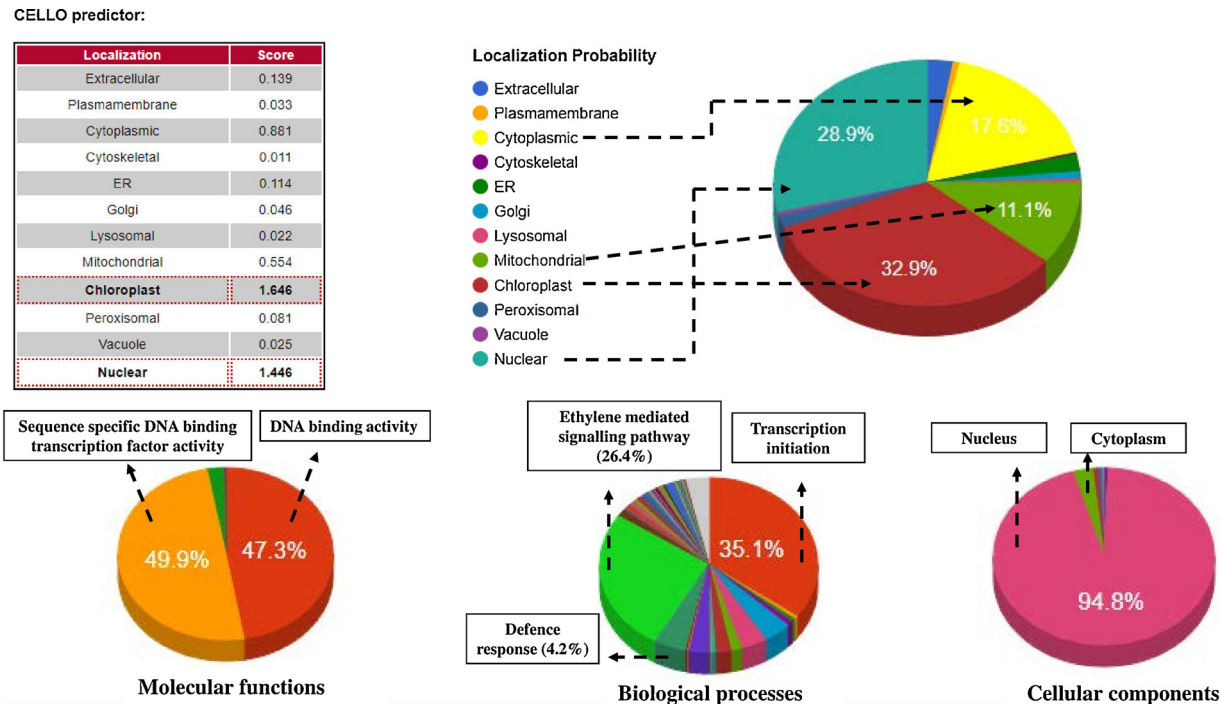

Fig. 12. The subcellular localization and functional gene annotation of SlDREB1 using CELLO2GO web server. The significant terms are represented in terms of their percentage contribution.

photosynthetic pigment was observed more in these two hybrids thus efficiently orchestrating complex molecular network of stress responsive genes that are involved in the regulation of stomatal response, enabling plants to adapt, survive and reproduce at desired rate (Martinez et al., 2018).The results of the present study also concluded that fruit width in tomato appears to less affected by salt compared to fruit length and so, fruit length/width ratio may be an important indicator for salt tolerance in tomatoes (Munns and Tester, 2008).

Under salt stress, the expression levels of stress responsive genes involved in oxidative defence response (DREB1, DREB2, DREB3), protein homeostasis (HSP, ZFP), and membrane protection (LEA, EF, ATP) were significantly up-regulated in all the salt stressed tomato hybrids compared to control plants (Fig. 1). However, no significant differences in the expression of these stress related genes were observed between salt-tolerant and susceptible parents under normal conditions, despite of their contrasting nature. The possible explanation behind the enhanced tolerance of tomato hybrids may be due cumulative effect of all stress responsive gens *viz.,* DREB, HSP, ZFP and EF efficiently prevented the accumulation of Na^+ and facilitating K^+ uptake that may contributed to less oxidative damage in the hybrids compared to their parents. In the present study, salt stress induce generation of membrane damage, stomatal closure and ROSs generation may have in turn up-regulated the expression of several other stress responsive genes that have rendered better ion/osmotic homeostasis and enzyme activities thereby minimizing salt-induced oxidative damage (Diaz-Vivancos et al., 2013). However, additional work is required to understand the molecular mechanism of DREB1 in salt tolerance in tomato plants in the future.

Several studies in the past recent years have also well documented similar pattern of expression of Dehydration responsive element binding (DREB) proteins across diverse range of abiotic stresses in different plant species as we have observed in the present study thus pinpointing its persistent and generic role in plant's abiotic stress tolerance (Yamaguchi-Shinozaki and Shinozaki, 2006). However, little information regarding factors and mechanisms controlling its expression under stress condition is present. Therefore, the present study also aims to decipher phylogenetic footprint, potential binding motifs, cis-regulatory binding sites involved in the regulation of the expression of DREB TFs along with identification of probable functional protein network modulating the expression of DREB1 TF at mRNA level in tomato.

In this study, the bootstrap phylogenetic investigation made for AP2/ERF domains of SlDREB1 protein members were classified into 4 groups i.e. A1-A4. The analysis revealed close evolutionary relationship among the different members of tomato family displaying monophyletic origin of SlDREB1 with its wild homologue *S. pimpenellifolium* and close relationship between *S. pennelli.* The phylogenetic analysis clearly indicates that grouping and sub-grouping for DREB1 protein with in different members of tomato family had occurred in the early stages of evolution of terrestrial plants (Nakano et al., 2006; Mizoi et al., 2012). This notion was further supported by the results of the multiple sequence alignment done for the DREB1 proteins which reveals the occurrence of similar KYRG domains in all the members of tomato family *viz., S. lycopersicum, S. Pimpenellifolium, S. Pennelli, S. tuberosum, C. annum and N. tabcum*. The strong conservation around the KYRG domain in closely related and divergent species indicate that least disturbances had occurred during the course of evolution which might be involved in the regulation of DREB1 TF under climate extremes (Vatansever et al., 2017). Furthermore, construction of circos plot based on the AP2/ERF domain amino acid sequences of the DREB1 protein derived from all the six members of solanaceous family unambiguously demonstrated that SlDREB1 probably have evolved from the common ancestors (Pan et al., 2012).

Transcription factors are generally characterized into specific clades by the presence of functionally conserved motifs present within and outside of the DNA binding domain (Nijhawan et al., 2008). Analysis of conserved motifs reflects the presence of conserved amino acid sequences capable of performing diverse biological functions, protein-protein interaction and DNA-protein interaction (Nakano et al., 2006). In the present study, we identified a set of binding motifs both in N-terminal and C-terminal domains controlling the expression of DREB1 TF by performing motif search based on multiple sequence alignment and phylogenetic foot printing analysis of orthologous sequences. We found that members of DREB1 tomato family contains two functional

regions, first, KYRG motif rich in basic and hydrophobic amino acids at N-terminal end which is specifically involve in the DNA binding activity (Akhtar et al., 2013).The second region contain conserved LAYD motif at C-terminal end which has been proposed to play a significant role in protein-protein interaction by forming amphipathic alpha helix structure and is also believed to regulate the DNA binding activity by changing the orientation of KYRG element (Dong et al., 2012; Wu et al., 2015). Several *in-silico* studies on stress responsive genes and TFs have revealed important function of combinatorial interaction between conserved motifs in the regulation of gene expression under stress conditions (Wu et al., 2015) thus corroborating the result of the present study. Recently, *in silico* characterization of DREB gene family has been reported in many plant species including *Brassica rapa* (Song et al., 2013), *Phyllostachys edulis* (Wu et al., 2015) and recently in *Musa acuminata* (Kuang et al., 2017).

Whole genome shotgun analysis for gene prediction usually involve genome-wide pattern analysis using programs like TBLASTN and BLAST-P (Wu et al., 2015). In the present study, the results of TBLASTN analysis revealing same functional domains in the query sequences are further subjected Fgenesh gene prediction analysis to infer coding sequences along with transcriptional start site (TSS) and poly A tail which was further confirmed by the BLAST results of uniprotKB database. Verification of desired functional domains of the query sequences after gene prediction analysis by various online protein family databases such as Pfam, SMART and HMMER has been widely reported (Finn et al., 2010; Letunic et al., 2012; Rustici et al., 2012). Fgenesh analysis strongly suggest the presence of several exon in the upstream region of DREB1 TF which may trigger the transcription activation of DREB1 under stress condition particularly with in 1 kb of gene promoter region (Sharoni et al., 2011). The functional relevance of which was further confirm by enhanced expression of DREB TFs in tomato plants under salt stress condition. In another study analysis of gene related to natural resistance-associated macrophage proteins in tomato revealed all whole genome shotgun sequences across the tomato genome and also predicted possible coding sequences, TSS and poly A sites (Meena et al., 2018) which corroborates the results of the present study.

The qualitative and quantitative analysis of protein 3D structures have become an imperative tool for detection of protein families, homolog/ortholog relations and functional classification (Madej et al., 2013). The predicted SlDREB1 models in the present study were superior in terms of Ramachandran plot, PROCHECK, VADAR, ProSA, ResProx and QMEAN analysis with respect to the crystal structures of respective templates. Several attempts have been made to characterize DREB proteins in Arabidopsis, rice, grapevine, popular, bamboo and mulberry (Rehman and Mahmood, 2015; Wu et al., 2015). However, few studies have reported and functionally characterize DREB proteins in tomato, so characterizing DREB1 protein both at structural and functional levels could reveal significant insight regarding their potential sites and catalytic residues required for providing abiotic stress tolerance in plants includingsalt stress. The DREB subfamily members in plants have been clustered into six groups A1-A6, of which A1 and A2 are the largest groups (Sakuma et al., 2002) and have been highly conserved throughout the evolution of terrestrial plants. Several studies have been performed for the prediction of structural and functional properties of proteins through computational approaches. For instance, Wu et al. (2015) and Liu et al. (2015) characterized the structural and functional attributes of bamboo and mulberry DREB genes and established their phylogenetic origin, diverseness and ancestral relationships. The functional attributes were evaluated through gene expression analysis followed by *in silico* analysis of functional domain and conserved motif signatures. Superimposition of the modelled protein structures with the available crystal structures of the respective templates help in the prediction of domain structures, structural constraint and topological details (Illergård et al., 2009). In the present study, the superimposition results of predicted model showed high similarity with 1GCC, 2GCC and 3GCC templates as compared 5WX9 which was confirmed by observed local and global RMSD values for each template indicated strong structural similarity despite of no sequence similarity between the predicted model and the templates thereby confirming the notion that proteins drifted apart during the course of evolution alsoexhibit strong structural constraints (Panchenko and Madej, 2005).

The DREB TFs have been shown to bind or interact preferentially by DRE elements (with core motif TACCGACAT) which are located in the promoter region of downstream genes that regulates dynamic signalling network via kinase and phosphorylation activities (Hichri et al., 2016). The functional domains and motifs located outside of the AP2/ERF domain strengthen the binding affinity of DREBs under varying climatic conditions (Hichri et al., 2016). The analysis of three-dimensional structure of AP2/ERF domain have revealed the importance conserved amino acid residues involved in DNA-protein interaction where presence of Val^{14} are Glu^{19} significantly increased DNA-binding activity (Sakuma et al., 2002; Akhtar et al., 2013). However, some of the studies on wheat, rice, barley and rye have reported non-conservation of Glu^{19} residue (Agarwal et al., 2006) and reported inferiority of Glu^{19} over Val^{14} for recognition and DNA binding activity in SlDREB1 proteins. Apart from Val^{14} are Glu^{19} other amino acids that are critical for DNA binding activity are Arg^{6}, Arg^{8}, Arg^{25} and Trp^{27} (Lata and Prasad, 2011) and in our results we have also found that along with Arg^{18}, Glu^{19} other amino acid residues *viz.,*Pro^{20}, Lys^{21}, Arg^{22}, Leu^{26}, Trp^{27}, Leu^{28}, Asp^{43}, Ala^{44}, Arg^{46}, Ala^{47}, Met^{48}, Tyr^{49}, Gly^{50}, Pro^{51}, Cys^{52}, and Arg^{54}indicates their significant role in binding to DRE element which may be involved in triggering defence response to environmental stress (Rao et al., 2015; Hichri et al., 2016). Recently, Rao et al. (2015) performed computational analysis and phylogenetically characterized DREB1 gene in wild tomato (*S. pimpinellifolium*) in response to salt stress and concluded that the expression of DREB1 gene is associated with enhanced salinity tolerance in wild as well as in cultivated tomato. However, future genome wide association studies will reveal neo-functionalization of different DREB genes implicated in salt tolerance in tomato.

The functional protein interactive network identified, characterized and predicted the proteins that were crucial for deciphering functional regulatory roles of DREB1 interactingproteinsboth at cellular and systemic levels and these predicted interactomes may act as probable sources to decipher protein-protein interaction of other species at genomic level (Yue et al., 2016). In our results, we have shown all the possible interacting partners that were making an interaction with the SlDREB1 protein through string server. SlDREB1 (Solyc06g050520.1.1) was found to be in interaction with only one protein *viz.,*diphthine ammonia ligase enzyme, an uncharacterized protein with possible role as eukaryotic elongation associated factor. From second shell interactors SlDREB1 displayed maximum interaction with score values of 0.913 and 0.878 with an uncharacterized protein (Solyc08g062910.2.1 andSolyc12g062900.1.1) having translation elongation factor activity and GTPase activity and lastly with ubiquitin binding like protein which are involved in metal ion binding. These protein-protein interaction studies unravelled all the possible interacting partners between SlDREB1 and other proteins from high to medium to low confidence levels showing direct/indirect partners involved in boosting plant innate immunity and related signalling pathways (Miller et al., 2016).

Gene ontology (GO) terms are descriptors of all the possible gene and related products that characterized them on the basis of three ontologies *viz.,* cellular, biological and molecular functions (Barnawal et al., 2016). In the present study, most significant GO terms under biological process were positive regulation of transcription (GO: 0045893), whereas, the most significant GO terms under molecular function were transcription factor activity (GO: 0003700). Cello2GO results showed localization of SlDREB1 protein to the chloroplast (32.9%) mostly involved in ethylene mediated signalling pathway, transcription initiation and defence response. Whereas, 28.9% of the SlDREB1 protein belongs to nucleus (score value 1.44) performing sequence specific DNA binding transcription factor activity and 17.6% of the SlDREB1 protein were localised in cytoplasm. In the past few years,

several studies have been conducted to decipher protein-protein interaction in response to several biotic and abiotic stress conditions. For instance, functional gene ontology analysis performed for tomato WRKY proteins also identified similar GO terms involved in biological process and molecular function (Aamir et al., 2017) involved in defence response, transcription activation and DNA binding. In another instance similar study was also conducted to decipher functional interactive partners associated with tomato NRAMP3 protein and defence response (Meena et al., 2018) which are in accordance with the results of the present study.

5. Conclusion

The present study concluded that exposure of hybrids to salt stress (400 mM) significantly affected membrane stability, photosynthetic activity, antioxidant defence system resulting in decreased average yield per plant. Hybrids *viz.,* VRTH-1754 and VRTH-1755 were able to ameliorate salinity induced oxidative damage by efficiently modulating their physiological, biochemical and molecular defence response and contriving salt induced oxidative stress. Furthermore, the expression data generated for several stress related genes along with DREBs revealed that the overexpression of DREB1 and DEEB2 genes can improve the salt tolerance in tomato plants. In addition, structural and functional characterization of SlDREB1 TFs through *in silico* approaches revealed that the SlDREB1 structure was highly conserved among the systems thereby confirming the notion that the structure is more conserved than the sequence which clearly demonstrate them to play identical roles across different taxa. Furthermore, computational analysis of SlDREB1proteins have provided necessary information about their phylogenetic origin, conserved motifs, functional interactive partners which will be helpful in tailoring plants with improved agronomical traits which will have the potential to endure under different abiotic stress conditions. Additionally, in the present work we have confirm that the key residues that make interaction more feasible and favourable with the DRE element is the KYRG region of AP2/ERF domain that efficiently regulate gene expression of stress responsive genes especially in tomato. Till date there is insufficient knowledge about the possible role of DREB TFs in abiotic stress tolerance in tomato and information generated in this study will surely expand our understanding of the complex regulatory networks associated with DREB1 proteins during stress response at vegetative stage and will open new possibilities in agriculture and allied sectors to achieve better yield under adverse environmental condition.

Conflict of interest

The authors declare no conflicts of interest.

Author's contributions

K.K.R., planned and conducted all the field,*in-vitro* experiments and *in-silico* analysis, wrote final draft of the manuscript; N.R., designed, planned and supervised the whole work; S.P.R., assisted in the interpretation of *in-silico* results, edited and prepared final draft of the manuscript.

Acknowledgements

This work is a part of ICAR-sponsored project "Consortium Research Platform for Hybrid Technology (Tomato)" funded by ICAR-Indian Agricultural Research Institute, New Delhi, India (Grant No: F.3/CRPHT/Gen/2015-16). We are also thankful to the Director, Indian Institute of Vegetable Research, Varanasi for providing necessary facilities for conducting the research and assistance to run this project smoothly. The authors are thankful to the ISLS, DST PURSE, and FIST program facility of the Department of Botany, BHU to carry out bioinformatics and molecular work.

Appendix A. Supplementary data

Supplementary material related to this article can be found, in the online version, at doi:https://doi.org/10.1016/j.envexpbot.2019.05.015.

References

Aamir, M., Singh, V.K., Meena, M., Upadhyay, R.S., Gupta, V.K., Singh, S., 2017. Structural and functional insights into WRKY3 and WRKY4 transcription factors to unravel the WRKY–DNA (W-Box) complex interaction in tomato (*Solanum lycopersicum* L.). A computational approach. Front. Plant Sci. 8, 819.

Agarwal, P.K., Agarwal, P., Reddy, M.K., Sopory, S.K., 2006. Role of DREB transcription factors in abiotic and biotic stress tolerance in plants. Plant Cell Rep. 25, 1263–1274.

Akhtar, M., Jaiswal, A., Jaiswal, J.P., Qureshi, M.I., Tufchi, M., Singh, N.K., 2013. Cloning and characterization of cold, salt and drought inducible C-repeat binding factor gene from a highly cold adapted ecotype of *Lepidium latifolium* L. Physiol. Mol. Biol. Plants 19 (2), 221–230.

Anjum, S.A., Xie, X.Y., Wang, L.C., Saleem, M.F., Man, C., Lei, W., 2011. Morphological, physiological and biochemical responses of plants to drought stress. Afr. J. Agric. Res. 6 (9), 2026–2032.

Arnon, D.I., 1949. Copper enzymes in isolated chloroplast. Polyphenoxidase in beta vulgaris. Plant Physiol. 24, 1–15.

Ashraf, M.F.M.R., Foolad, M., 2007. Roles of glycine betaine and proline in improving plant abiotic stress resistance. Environ. Exp. Bot. 59 (2), 206–216.

Ashraf, M.P.J.C., Harris, P.J.C., 2004. Potential biochemical indicators of salinity tolerance in plants. Plant Sci. 166 (1), 3–16.

Bailey, T.L., Williams, N., Misleh, C., Li, W.W., 2006. MEME: discovering and analyzing DNA and protein sequence motifs. Nucleic Acids Res. 34, W369–W373.

Barnawal, V.K., Negi, N., Khorana, P., 2016. Genome-wide identification and structural, functional and evolutionary analysis of WRKY components of mulberry. Sci. Rep. 6, 30794.

Bates, L.S., Waldren, R.P., Teare, I.D., 1973. Rapid determination of free proline for water-stress studies. Plant Soil 39, 205–207.

Benkert, P., Kunzli, M., Schwede, T., 2009. QMEAN server for protein model quality estimation. Nucleic Acids Res. 37, W510–W514.

Berman, H.M., Westbrook, J., Feng, Z., Gilliland, G., Bhat, T.N., Weissig, H., et al., 2000. The protein data bank. Nucleic Acids Res. 28, 235–242.

Bian, S., Jiang, Y., 2009. Reactive oxygen species, antioxidant enzyme activities and gene expression patterns in leaves and roots of Kentucky bluegrass in response to drought stress and recovery. Sci. Hortic. 120 (2), 264–270.

Bita, C., Gerats, T., 2013. Plant tolerance to high temperature in a changing environment: scientific fundamentals and production of heat stress-tolerant crops. Front. Plant Sci. 4, 273.

Castrignano, T., De Meo, P.D., Cozzetto, D., Talamo, I.G., Tramontano, A., 2006. The PMDB protein model database. Nucleic Acids Res. 34, D306–D309.

Charfeddine, M., Saïdi, M.N., Charfeddine, S., Hammami, A., Bouzid, R.G., 2015. Genome-wide analysis and expression profiling of the ERF transcription factor family in potato (*Solanum tuberosum* L.). Mol. Biotechnol. 57 (4), 348–358.

Chen, H., Liu, L., Wang, L., Wang, S., Cheng, X., 2016. VrDREB2A, a DREB-binding transcription factor from *Vigna radiata*, increased drought and high-salt tolerance in transgenic Arabidopsis thaliana. J. Plant Res. 129 (2), 263–273.

Colovos, C., Yeates, T.O., 1993. ERRAT: an empirical atom-based method for validating protein structures. Protein Sci. 2, 1511–1519.

DaCosta, M., Huang, B., 2007. Changes in antioxidant enzyme activities and lipid peroxidation for bentgrass species in response to drought stress. J. Am. Soc. Hortic. Sci. 132 (3), 319–326.

Das, S., Lee, D., Sillitoe, I., Dawson, N.L., Lees, J.G., Orengo, C.A., 2016. Functional classification of CATH superfamilies: a domain-based approach for protein function annotation. Bioinformatics 32, 2889.

de Castro, E., Sigrist, C.J.A., Gattiker, A., Bulliard, V., Langendijk-Genevaux, P.S., Gasteiger, E., et al., 2006. ScanProsite: detection of PROSITE signature matches and ProRule-associated functional and structural residues in proteins. Nucleic Acids Res. 1, 362–365.

Deshmukh, P.S., Sairam, R.K., Shukla, D.S., 1991. Measurement of ion leakage as a screening technique for drought resistance in wheat phenotypical groups. Indian J. Plant Physiol. 34, 89–91.

Dey, S., Corina Vlot, A., 2015. Ethylene responsive factors in the orchestration of stress responses in monocotyledonous plants. Front. Plant Sci. 6, 640.

Diaz-Vivancos, P., Faize, M., Barba-Espin, G., Faize, L., Petri, C., Hernández, J.A., Burgos, L., 2013. Ectopic expression of cytosolic superoxide dismutase and ascorbate peroxidase leads to salt stress tolerance in transgenic plums. Plant Biotechnol. J. 11 (8), 976–985.

Dong, W., Ai, X., Xu, F., Quan, T., Liu, S., Xia, G., 2012. Isolation and characterization of a bread wheat salinity responsive ERF transcription factor. Gene 511 (1), 38–45.

Erskine, W., Upadhyaya, H.D., Malik, A.I., 2014. Salinity. In: Jackson, M., Ford-Lloyd, B., Parry, M. (Eds.), Plant Genetic Resources and Climate Change. CAB International, Oxfordshire, UK, pp. 236–250.

Fernandez-Garcia, N., Olmos, E., Bardisi, E., García-De la Garma, J., López-Berenguer, C., Rubio-Asensio, J.S., 2014. Intrinsic water use efficiency controls the adaptation to high salinity in a semi-arid adapted plant, henna (*Lawsoniainermis* L.). J. Plant

Physiol. 171 (5), 64–75.
Finn, R.D., Mistry, J., Tate, J., Coggill, P., Heger, A., Pollington, J.E., Gavin, O.L., Gunasekaran, P., Ceric, G., et al., 2010. The Pfam protein families database. Nucleic Acids Res. 38 (Database issue), D211–222.
Gomez-Bellot, M.J., Alvarez, S., Banon, S., Ortuno, M.F., Sanchez-Blanco, M.J., 2013. Physiological mechanisms involved in the recovery of euonymus and laurustinus subjected to saline waters. Agric. Water Manage. 128, 131–139.
Guo, M., Liu, J.H., Ma, X., Luo, D.X., Gong, Z.H., Lu, M.H., 2016. The plant heat stress transcription factors (HSFs): structure, regulation, and function in response to abiotic stresses. Front. Plant Sci. 9 (7), 114.
Hall, T.A., 1999. BioEdit: a user-friendly biological sequence alignment editor and analysis program for Windows 95/98/NT. Nucleic Acids Symp. Ser. 41, 95–98.
Heath, R.L., Packer, L., 1968. Photoperoxidation in isolated chloroplasts. Kinetics and stoichiometry of fatty acid peroxidation. Arch. Biochem. Biophys. 125, 189–198.
Hessini, K., Martínez, J.P., Gandour, M., Albouchi, A., Soltani, A., Abdelly, C., 2009. Effect of water stress on growth, osmotic adjustment, cell wall elasticity and water-use efficiency in Spartina alterniflora. Environ. Exp. Bot. 67 (2), 312–319.
Hichri, I., Muhovski, Y., Clippe, A., Zizkova, E., Dobrev, P.I., Motyka, V., Lutts, S., 2016. SlDREB2, a tomato dehydration-responsive element-binding 2 transcription factor, mediates salt stress tolerance in tomato and Arabidopsis. Plant Cell Environ. 39 (1), 62–79.
Hichri, I., Muhovski, Y., Zizkova, E., Dobrev, P.I., Franco-Zorilla, J.M., Solano, R., Lutts, S., 2014. The *Solanum lycopersicum* Zinc Finger-2 cysteine-2/ histidine-2 repressor-like transcription factor regulates development and tolerance to salinity in tomato and Arabidopsis. Plant Physiol. 164, 1967–1990.
Hu, B., Jin, J., Guo, A.Y., Zhang, H., Luo, J., Gao, G., 2014. GSDS 2.0: an upgraded gene feature visualization server. Bioinformatics 31 (8), 1296–1297.
Huang, B., 2009. MetaPocket: a meta approach to improve protein ligand binding site prediction. OMICS 13 (4), 325–330.
Ikbal, F.E., Hernández, J.A., Barba-Espín, G., Koussa, T., Aziz, A., Faize, M., Diaz-Vivancos, P., 2014. Enhanced salt-induced antioxidative responses involve a contribution of polyamine biosynthesis in grapevine plants. J. Plant Physiol. 171 (10), 779–788.
Illergård, K., Ardell, D.H., Elofsson, A., 2009. Structure is three to ten times more conserved than sequence: a study of structural response in protein cores. Proteins 77, 499–508.
Jana, S., Choudhuri, M.A., 1981. Glycolate metabolism of three submerged aquatic angiosperm during aging. Aquat. Bot. 12, 345–354.
Jones, P., Binns, D., Chang, H.Y., Fraser, M., Li, W., McAnulla, C., et al., 2014. InterProScan 5: genome-scale protein function classification. Bioinformatics 30, 1236–1240.
Kazan, K., 2015. Diverse roles of jasmonates and ethylene in abiotic stress tolerance. Trends Plant Sci. 20 (4), 219–229.
Krzywinski, M., Schein, J., Birol, I., Connors, J., Gascoyne, R., Horsman, D., et al., 2009. Circos: an information aesthetic for comparative genomics. Genome Res. 19, 1639–1645.
Kuang, J.F., Chen, J.Y., Liu, X.C., Han, Y.C., Xiao, Y.Y., Shan, W., Tang, Y., Wu, K.Q., He, J.X., Lu, W.J., 2017. The transcriptional regulatory network mediated by banana (*Musa acuminata*) dehydration-responsive element binding (MaDREB) transcription factors in fruit ripening. New Phytol. 214 (2), 762–781.
Laskowski, R.A., Chistyakov, V.V., Thornton, J.M., 2005. PDBsum more: new summaries and analyses of the known 3D structures of proteins and nucleic acids. Nucleic Acids Res. 1, D266–D268.
Lata, C., Prasad, M., 2011. Role of DREBs in regulation of abiotic stress responses in plants. J. Exp. Bot. 62, 4731–4748.
Letunic, I., Doerks, T., Bork, P., 2012. SMART 7: recent updates to the protein domain annotation resource. Nucleic Acids Res. 40, 302–305.
Liu, C., Liu, Y., Guo, K., Fan, D., Li, G., Zheng, Y., Yu, L., Yang, R., 2011. Effect of drought on pigments, osmotic adjustment and antioxidant enzymes in six woody plant species in karst habitats of southwestern China. Environ. Exp. Bot. 71 (2), 174–183.
Liu, X.Q., Zhu, J.J., Wei, C.J., Guo, Q., Bian, C.K., Xiang, Z.H., Zhao, A.C., 2015. Genome-wide identification and characterization of the DREB transcription factor gene family in mulberry. Biol. Plant. 59 (2), 253–265.
Livak, K.J., Schmittgen, T.D., 2001. Analysis of relative gene expression data using real-time quantitative PCR and the $2^{-\Delta\Delta Ct}$ method. Methods 25, 402–408.
Lovell, S.C., Davis, I.W., Arendall, W.B., de Bakker, P.I., Word, J.M., Prisant, M.G., et al., 2003. Structure validation by Ca geometry: phi-psi and C-beta deviation. Proteins 50, 437–450.
Macindoe, G., Mavridis, L., Venkatraman, V., Devignes, M., Ritchie, D., 2010. Hex Server: an FFT-based protein docking server powered by graphics processors. Nucleic Acids Res. 38, W445–W449.
Madej, T., Lanczycki, C.J., Zhang, D., Thiessen, P.A., Geer, R.C., Marchler-Bauer, A., Bryant, S.H., 2013. MMDB and VAST+: tracking structural similarities between macromolecular complexes. Nucleic Acids Res. 42 (D1), D297–D303.
Maiti, R., Van Domeselaar, G.H., Zhang, H., Wishart, D.S., 2004. SuperPose: a simple server for sophisticated structural superposition. Nucleic Acids Res. 32, W590–W594.
Marchler-Bauer, A., Lu, S., Anderson, J.B., Chitsaz, F., Derbyshire, M.K., DeWeese-Scott, C., et al., 2011. CDD: a Conserved Domain Database for the functional annotation of proteins. Nucleic Acids Res. 39, D225–D229.
Martinez, V., Nieves-Cordones, M., Lopez-Delacalle, M., Rodenas, R., Mestre, T.C., Garcia-Sanchez, F., Rubio, F., Nortes, P.A., Mittler, R., Rivero, R.M., 2018. Tolerance to stress combination in tomato plants: new insights in the protective role of melatonin. Molecules 23 (3), 535.
McKersie, B.D., Hoekstra, F., Krieg, L., 1990. Differences in the susceptibility of plant membrane lipids to peroxidation. Biochim. Biophys. Acta 1030, 119–126.
Meena, M., Aamir, M., Kumar, V., Swapnil, P., Upadhyay, R.S., 2018. Evaluation of morpho-physiological growth parameters of tomato in response to Cd induced toxicity and characterization of metal sensitive NRAMP3 transporter protein. Environ. Exp. Bot. 148, 144–167.
Miller, J.C., Chezem, W.R., Clay, N.K., 2016. Ternary WD 40 repeatcontaining protein complexes: evolution, composition and roles in plant immunity. Front. Plant Sci. 6, 1108.
Mishra, S., Phukan, U.J., Tripathi, V., Singh, D.K., Luqman, S., Shukla, R.K., 2015. PsAP2 an AP2/ERF family transcription factor from *Papaver somniferum* enhances abiotic and biotic stress tolerance in transgenic tobacco. Plant Mol. Biol. 89 (1-2), 173–186.
Mizoi, J., Shinozaki, K., Yamaguchi-Shinozaki, K., 2012. AP2/ERF family transcription factors in plant abiotic stress responses. BBA-Gene Reg. Mech. 1819 (2), 86–96.
Muchate, N.S., Nikalje, G.C., Rajurkar, N.S., Suprasanna, P., Nikam, T.D., 2016. Plant salt stress: adaptive responses, tolerance mechanism and bioengineering for salt tolerance. Bot. Rev. 82 (4), 371–406.
Muneer, S., Jeong, B.R., 2019. Proteomic analysis of salt-stress responsive proteins in roots of tomato (*Lycopersiconesculentum* L.) plants towards silicon efficiency. Plant Growth Regul. 77 (2), 133–146.
Munns, R., Gilliham, M., 2015. Salinity tolerance of crops–what is the cost? New Phytol. 208 (3), 668–673.
Munns, R., Tester, M., 2008. Mechanisms of salinity tolerance. Annu. Rev. Plant Biol. 59, 651–681.
Nakano, T., Suzuki, K., Fujimura, T., Shinshi, H., 2006. Genome-wide analysis of the ERF gene family in Arabidopsis and rice. Plant Physiol. 140 (2), 411–432.
Nazar, R., Iqbal, N., Masood, A., Syeed, S., Khan, N.A., 2011. Understanding the significance of sulfur in improving salinity tolerance in plants. Environ. Exp. Bot. 70 (2-3), 80–87.
Nijhawan, A., Jain, M., Tyagi, A.K., Khurana, J.P., 2008. Genomic survey and gene expression analysis of the basic leucine zipper transcription factor family in rice. Plant Physiol. 146 (2), 333–350.
Pan, Y., Seymour, G.B., Lu, C., Hu, Z., Chen, X., Chen, G., 2012. An ethylene response factor (ERF5) promoting adaptation to drought and salt tolerance in tomato. Plant Cell Rep. 31 (2), 349–360.
Panchenko, A.R., Madej, T., 2005. Structural similarity of loops in protein families: toward the understanding of protein evolution. BMC Evol. Biol. 5 (1), 10.
Pandey, B., Sharma, P., Saini, M., Pandey, D.M., Sharma, I., 2014. Isolation and characterization of dehydration responsive element-binding factor 2 (DREB2) from Indian wheat (*Triticum aestivum* L.) cultivars. Aust. J. Crop Sci. 8, 44–54.
Park, H.J., Kim, W.Y., Yun, D.J., 2016. A new insight of salt stress signaling in plant. Mol. Cells 39 (6), 447.
Porra, R.J., Thompson, W.A., Kriedemann, P.E., 1989. Determination of accurate extinction coefficients and simultaneous equations for assaying chlorophylls a and b extracted with four different solvents: verification of the concentration of chlorophyll standards by atomic absorption spectroscopy. Biochim. Biophys. Acta 975, 384–394.
Rao, G., Sui, J., Zeng, Y., He, C., Zhang, J., 2015a. Genome-wide analysis of the AP2/ERF gene family in Salix arbutifolia. FEBS Open Biol. 5, 132–137.
Rao, E.S., Kadirvel, P., Symonds, R.C., Geethanjali, S., Thontadarya, R.N., Ebert, A.W., 2015. Variations in DREB1A and VP1. 1 genes show association with salt tolerance traits in wild tomato (*Solanum pimpinellifolium*). PloS One 10 (7), e0132535.
Rehman, S., Mahmood, T., 2015. Functional role of DREB and ERF transcription factors: regulating stress-responsive network in plants. Acta Physiol. Plant. 37 (9), 178.
Rustici, G., Kolesnikov, N., Brandizi, M., Burdett, T., Dylag, M., Emam, I., Farne, A., Hastings, E., Ison, J., Keays, M., Kurbatova, N., 2012. ArrayExpress update—trends in database growth and links to data analysis tools. Nucleic Acids Res. 41 (D1), D987–D990.
Sakuma, Y., Liu, Q., Dubouzet, J.G., Abe, H., Shinozaki, K., Yamaguchi-Shinozaki, K., 2002. DNA-binding specificity of the ERF/AP2 domain of Arabidopsis DREBs, transcription factors involved in dehydration-and cold-inducible gene expression. Biochem. Biophys. Res. Commun. 290 (3), 998–1009.
Shabala, S., Munns, R., 2017. Salinity stress: physiological constraints and adaptive mechanisms. Plant Stress Physiology, 2nd ed. CABI, Wallingford, pp. 24–63.
Shahi, S.K., Singh, V.K., Kumar, A., Gupta, S.K., Singh, S.K., 2013. Interaction of dihydrofolate reductase and aminoglycoside adenyl transferase enzyme from *Klebsiella pneumoniae* multidrug resistant strain DF12SA with clindamycin: a molecular modeling and docking study. J. Mol. Model. 19, 973–983.
Sharoni, A.M., Nuruzzaman, M., Satoh, K., Shimizu, T., Kondoh, H., Sasaya, T., Choi, I.-R., Omura, T., Kikuchi, S., 2011. Gene structures, classification and expression models of the AP2/EREBP transcription factor family in rice. Plant Cell Physiol. 52, 344–360.
Sillitoe, I., Lewis, T.E., Cuff, A., Das, S., Ashford, P., Dawson, N.L., et al., 2015. CATH: comprehensive structural and functional annotations for genome sequences. Nucleic Acids Res. 43, D376–D381.
Singh, A., Kaushik, R., Mishra, A., Shanker, A., Jayaram, B., 2016. ProTSAV: a protein tertiary structure analysis and validation server. BBA-Proteins Proteom. 1864 (1), 11–19.
Song, X., Li, Y., Hou, X., 2013. Genome-wide analysis of the AP2/ERF transcription factor superfamily in Chinese cabbage (*Brassica rapa* ssp. pekinensis). BMC Genomics 14 (1), 573.
Solovyev, V., Kosarev, P., Seledsov, I., Vorobyev, D., 2006. Automatic annotation of eukaryotic genes, pseudogenes and promoters. Genome Biol. 7 10.1-10.12.
Sun, X.C., Gao, Y.F., Li, H.R., Yang, S.Z., Liu, Y.S., 2015. Over-expression of SlWRKY39 leads to enhanced resistance to multiple stress factors in tomato. J. Plant Biol. 58 (1), 52–60.
Supek, F., Bošnjak, M., Škunca, N., Šmuc, T., 2011. REVIGO summarizes and visualizes long lists of gene ontology terms. PloS One 6 (7), e21800.
Szklarczyk, D., Franceschini, A., Wyder, S., Forslund, K., Heller, D., HuertaCepas, J., et al., 2015. STRING v10: protein–protein interaction networks, integrated over the tree of life. Nucleic Acids Res. 43, D447–D452.

Tamura, K., Stecher, G., Peterson, D., Filipski, A., Kumar, S., 2013. MEGA6: molecular evolutionary genetics analysis version 6.0. Mol. Biol. Evol. 30, 2725–2729.
Tang, X., Mu, X., Shao, H., Wang, H., Brestic, M., 2015. Global plant-responding mechanisms to salt stress: physiological and molecular levels and implications in biotechnology. Crit. Rev. Biotechnol. 35 (4), 425–437.
Tounekti, T., Vadel, A.M., Oñate, M., Khemira, H., Munné-Bosch, S., 2011. Salt-induced oxidative stress in rosemary plants: damage or protection? Environ. Exp.Bot. 71 (2), 298–305.
Turner, N.C., Kramer, P.J., 1980. In: Turner, N.C., Kramer, P.J. (Eds.), Adaptation of Plants to Water and High Temperature Stress. Wiley Interscience, New York p. ix–x. (Intro.).
Vatansever, R., Uras, M.E., Sen, U., Ozyigit, I.I., Filiz, E., 2017. Isolation of a transcription factor DREB1A gene from *Phaseolus vulgaris* and computational insights into its characterization: protein modeling, docking and mutagenesis. J. Biomol. Struct. Dyn. 35 (14), 3107–3118.
Wang, H., Wang, H., Shao, H., Tang, X., 2016. Recent advances in utilizing transcription factors to improve plant abiotic stress tolerance by transgenic technology. Front. Plant Sci. 7, 67.
Wiederstein, M., Sippl, M.J., 2007. ProSA-web: interactive web service for the recognition of errors in three-dimensional structures of proteins. Nucleic Acids Res. 35, W407–W410.
Willard, L., Ranjan, A., Zhang, H., Monzavi, H., Boyko, R.F., Sykes, B.D., Wishart, D.S., 2003. VADAR: a web server for quantitative evaluation of protein structure quality. Nucleic Acids Res. 31 (13), 3316–3319.
Wu, H., Lv, H., Li, L., Liu, J., Mu, S., Li, X., Gao, J., 2015. Genome-wide analysis of the AP2/ERF transcription factors family and the expression patterns of DREB genes in Moso Bamboo (*Phyllostachys edulis*). Plos One 10 (5), e0126657.
Xin, S., Yu, G., Sun, L., Qiang, X., Xu, N., Cheng, X., 2014. Expression of tomato SlTIP2;2 enhances the tolerance to salt stress in transgenic Arabidopsis and interacts with target proteins. J. Plant Res. 127, 659–708.
Xu, D., Zhang, Y., 2011. Improving the physical realism and structural accuracy of protein models by a two-step atomic-level energy minimization. Biophys. J. 101 (10), 2525–2534.
Xu, X., Yang, F.A.N., Xiao, X., Zhang, S., Korpelainen, H., Li, C., 2008. Sex-specific responses of *Populuscathayana* to drought and elevated temperatures. Plant Cell Environ. 31 (6), 850–860.
Yamaguchi-Shinozaki, K., Shinozaki, K., 2006. Transcriptional regulatory networks in cellular responses and tolerance to dehydration and cold stresses. Annu. Rev. Plant Biol. 57 781-80.
Yu, C.S., Cheng, C.W., Su, W.C., Chnag, K.C., Huang, S.W., Hwang, J.K., et al., 2014. CELLO2GO: a web server for protein subcellular localization prediction with functional gene ontology annotation. PLoS One 9, e99368.
Yue, J., Xu, W., Ban, R., Hunag, S., Miao, M., Tang, X., et al., 2016. PTIR: predicted tomato interactome resource. Sci. Rep. 6, 25047.